Validation of Pressure Reactivity and Pulse Amplitude Indices Against the Lower Limit of Autoregulation, Part I: Experimental Intra-Cranial Hypertension

Frederick A. Zeiler,[1-3] Joseph Donnelly,[4] Leanne Calviello,[4] Jennifer K. Lee,[5] Peter Smielewski,[4] Ken Brady,[7] Dong-Joo Kim,[8] Marek Czosnyka[4,6]

1. Division of Anaesthesia, Addenbrooke's Hospital, University of Cambridge, Cambridge, UK
2. Section of Surgery, Rady Faculty of Health Sciences, University of Manitoba, Winnipeg, Canada
3. Clinician Investigator Program, Rady Faculty of Health Science, University of Manitoba, Winnipeg, Canada
4. Section of Brain Physics, Division of Neurosurgery, Addenbrooke's Hospital, University of Cambridge, Cambridge, UK
5. Department of Anesthesiology and Critical Care Medicine, Baltimore, Maryland, USA
6. Institute of Electronic Systems, Warsaw University of Technology, Warsaw, Poland
7. Pediatric Cardiology, Texas Children's Hospital, Baylor College of Medicine, USA
8. Department of Brain and Cognitive Engineering, Korea University, Seoul, South Korea

Corresponding Author:

Frederick A. Zeiler BSc MD FRCSC (Neurosurgery)
Section of Surgery
Rady Faculty of Health Sciences
University of Manitoba
Winnipeg, MB, Canada
Email: umzeiler@myumanitoba.ca

Contributing Authors:

Joseph Donnelly MBChB
Brain Physics Laboratory
Department of Clinical Neurosciences
Division of Neurosurgery
University of Cambridge
Email: donnellyj87@gmail.com

Leanne Calviello BA MSc
Brain Physics Laboratory
Division of Neurosurgery
Dept of Clinical Neurosciences
University of Cambridge
Email: lac76@cam.ac.uk

Jennifer K. Lee MD
Associate Professor
Department of Anesthesiology and Critical Care
Johns Hopkins University
Baltimore, Maryland, USA
Email: jennifer.lee@jhmi.edu

Peter Smielewski PhD
Senior Research Associate
Brain Physics Laboratory
Department of Clinical Neurosciences
Division of Neurosurgery
University of Cambridge
Email: ps10011@cam.ac.uk

Ken Brady MD
Associate Professor
Department of Anesthesiology
Baylor College of Medicine
Houston, TX, USA
Email: ken.brady@me.com

Dong-Joo Kim, PhD
Associate Professor
Department of Brain & Cognitive Engineering
Korea University, Seoul, South Korea,
E-mail: dongjookim@korea.ac.kr

Marek Czosnyka PhD
Professor of Brain Physics
Brain Physics Laboratory
Department of Clinical Neurosciences
Division of Neurosurgery
University of Cambridge
Cambridge, UK
CB2 0QQ
Email: mc141@medschl.cam.ac.uk

Abstract:

To provide validation of intracranial pressure (ICP) derived continuous indices of cerebrovascular reactivity against the lower limit of autoregulation (LLA). Utilizing an intra-cranial hypertension model within white New Zealand rabbits, ICP, TCD, laser Doppler flowmetry (LDF) and arterial blood pressure were recorded. Data was retrospectively analyzed in a cohort of 12 rabbits with adequate signals for interrogating the LLA. We derived continuous indices of cerebrovascular reactivity: PRx (correlation between ICP and mean arterial pressure (MAP)), PAx (correlation between pulse amplitude of ICP (AMP) and MAP), and Lx (correlation between LDF based cerebral blood flow (CBF) and CPP). LLA was derived via piecewise linear regression of CPP vs. LDF or CPP vs. FVs plots. We then produced error bar plots for PRx, PAx, and Lx against 2.5 mm Hg bins of CPP, to display the relationship between these indices and the LLA. We compared the CPP values at clinically relevant thresholds of PRx and PAx, to the CPP defined at the LLA. ROC analysis was performed for each index across the LLA using 2.5 mm Hg bins for CPP. The mean LLA was 51.5 +/- 8.2 mm Hg. PRx and PAx error bar plots demonstrate that each index correlates with the LLA, becoming progressively more positive below the LLA. Similarly, CPP values at clinically relevant thresholds of PRx and PAx, were not statistically different from the CPP derived at the LLA. Finally, ROC analysis indicated that PRx and PAx predicted the LAA, with AUC's 0.795 (95% CI: 0.731 – 0.857, $p<0.0001$), 0.703 (95% CI: 0.631 – 0.775, $p<0.0001$), respectively. Both PRx and PAx generally

agree with LLA within this experimental model of intracranial hypertension. Further analysis of clinically used indices of autoregulation across the LLA within pure arterial hypotension models is required.
Keywords: Autoregulation, Continuous indices, Experimental, Validation, Lower Limit Autoregulation

Introduction:

Continuous measures of cerebrovascular reactivity have emerged as a means to monitor cerebral autoregulation within the intensive care unit (ICU).[1] These indices are derived via comparing slow wave fluctuations in a marker of pulsatile cerebral blood volume (CBV) or cerebral blood flow (CBF), with slow wave fluctuations in a driving pressure, such as cerebral perfusion pressure (CPP), or mean arterial pressure (MAP) [1,2] To date, number of papers have been published providing the link between these indices and patient outcome in a variety of neuro-pathologic states, including traumatic brain injury (TBI).[1-3]

Various multi-modal monitoring (MMM) devices are employed to provide a surrogate measure for slow fluctuation of CBV or CBF.[1] These monitored variables include, but are not limited to: intracranial pressure (ICP) and transcranial Doppler (TCD) based cerebral blood flow velocity (CBFV). Through the derivation of moving Pearson correlation coefficients between these surrogates of slow waves of CBV or CBF, and either MAP or CPP, one can produce continuously updating variables related to cerebrovascular reactivity.[1] Pressure reactivity index (PRx), the correlation between ICP and MAP, is the most widely quoted index within the literature, with the general view that negative values denoting "intact" autoregulation and positive values denoting "impaired" autoregulation.[1] Further, robust literature supports the association between "impaired" autoregulation (via PRx) and poor patient outcome in TBI,[1,4] with well-defined critical thresholds for PRx in existence.[5] Similar literature exists for the TCD derived indices: mean flow index (Mx – correlation between mean flow velocity (FVm) and CPP),[6] and systolic flow index (Sx – correlation between systolic flow velocity (FVs) and CPP).[7] Finally, less commonly quoted ICP derived indices, pulse amplitude index (PAx – correlation between pulse

amplitude of ICP (AMP) and MAP) and RAC (correlation between AMP and CPP), also seem to display strong correlations with outcome in TBI.[8]

Aside from literature supporting an association between these continuous measures and patient outcome, there is a paucity of data to support that these indices "respect" the limits of autoregulation (ie. become progressively more positive when CPP decreases below the LLA). To date, only PRx and two near infrared spectroscopy (NIRS) derived indices (COx and HVx) have been validated against the lower limit of autoregulation (LLA) in an animal model of arterial hypotension.[9,10] Thus, it is unknown as to whether the other ICP indices measure the LLA. Furthermore, there has yet to be confirmatory evidence to support that PRx does indeed measure the LLA. In addition, these continuous indices have never been validated against the LLA in a model of sustained intra-cranial hypertension, a physiologic event of importance in TBI. Thus, we will explore the correlation between PRx, PAx and RAC with the LLA in two experimental models of CPP reduction, in a 2-part manuscript series.

Within this manuscript, Part I, we will explore PRx, PAx and RAC within a model of sustained intra-cranial hypertension. The goal of this retrospective experimental study was twofold:

- Provide validation for PRx against the LLA in intracranial hypertension model.
- Explore whether other ICP derived indices (PAx, RAC) correlate with the LLA in this model.

Methods:

Animals and Ethics

The animals described within this study have in part been described in previous studies related the physiologic response to intra-cranial hypertension.[11,12] The archived data from a subset of 12 animals from these previous studies was utilized for the analysis. The initial experiments were conducted between 1995 and 1996, in accordance with the standards of the UK Animals Scientific Procedures act of 1986, under a UK home office license and with permission form the institutional animal care and use committee at the University of Cambridge. This has been previously documented.[11] Formal assessment of the LLA and its association with continuous indices of cerebrovascular reactivity using this dataset has not been previously conducted. Thus, this data was retrospectively analyzed for this purpose.

The initial study protocol has been previously described.[11,12] Twenty-eight white New Zealand (NZ) rabbits (7 female, 21 male; weight 2.7 – 3.7 kg) were subjected to cerebrospinal fluid (CSF) infusions. No adverse events were recorded within this animal cohort. As with previous publications on this animal cohort, experiments are reported in compliance with the ARRIVE guidelines for the reporting of animal experiments.[13]

These animals were placed under general anesthetic via alphaxalone/alphadalone induction, with 1-3% halothane in 3:1 nitrous oxide/oxygen maintenance. Each animal subsequently had ligation of the common carotid arteries, leaving the brain entirely basilar artery dependent and allowing for TCD assessment of global blood flow. Once 2 weeks had passed, the animals were placed under general anesthestic again, with cannulation of the jugular vein and placement of a tracheostomy. Arterial blood pressure (ABP) was measured through in the dorsal aorta after catheter insertion in the femoral artery (GaelTec, Dunvegan, UK). Cerebral blood velocity was measured using an 8MHz Doppler ultrasound

probe (PCDop 842, SciMed, Bristol, UK) positioned to insonate in the direction of the basilar artery through a burr hole located over the bregma. TCD ultrasonography was conducted from this point with the probe situated on the dura, facing the basilar artery. The TCD probe was held in situ with a custom-made holder, to reduce the chance of loss of insonation angle and signal. ICP was monitored using an intraparenchymal microsensor (Codman and Shurtleff, Raynham, MA, USA) inserted through a right frontal burr-hole, and a laser Doppler flowmetry (LDF) probe was placed epidurally through a further right frontal burr-hole (Moor Instruments, Axbridge, Devon, UK).

A lumbar laminectomy was performed to allow the positioning of a permanent catheter (sealed with cyanoacrylate after introduction) into the lumbar subarachnoid space. This facilitated the controlled infusion of artificial cerebrospinal fluid during the experimental protocol. Rectal temperature was monitored and the animals were placed on a padded warming blanket. The rabbits were given an intravenous infusion of pancuronium (pavulon, 0.5 mg/kg/h) and ventilation was controlled according to arterial pCO_2 via periodic arterial blood gas analyses. The animals were supported in the Sphinx position using a purpose-built head frame with three-point skull fixation. All experiments were performed in an animal laboratory at the same time of day.

CSF Infusion Protocol

The protocol for CSF infusion is identical to that previously reported.[11,12] After completion of the lumber laminectomy, the animals were allowed to rest for 20 minutes, with 5 minutes of baseline data recorded. Subsequently, the animals were subjected to raised ICP secondary to CSF infusion with Hartmanns solution into the lumbar cistern. Infusion rates were initially 0.1 mL/min, allowing ICP increase to reach a plateau of around 40 mm Hg after approximately 10 min. Thereafter the infusion rate was increased to rates between 0.2 and 2 mL/min to produce severe intra-cranial hypertension. ICP

was increased until the point where TCD diastolic flow velocity approached zero, which corresponded to an ICP of between 60 and 100mm Hg (mean 75mm Hg) at the termination of the experiment. Rabbits were euthanized with thiopental at the conclusion of the test. No direct pCO_2 manipulations occurred during this experiment, with a mean pCO_2 of 26.6 +/- 5.7 mm Hg seen across the cohort animals. Further details can be found in the previous studies reporting these experiments.[11,12]

Data Acquisition

All signals from the combined above invasive and non-invasive monitoring modalities were recorded and archived for future retrospective use. All recorded signals were digitized via an A/D converter (DT300; Data Translation, Marlboro, MA), sampled at frequency of 100 Hertz (Hz), using WREC software (Warsaw University of Technology) and subsequently processed using ICM+ software (Cambridge Enterprise Ltd, Cambridge, UK, http://icmplus .neurosurg.cam.ac.uk). Signal artifact was removed prior to further processing or analysis using tools available in ICM+.

Signal Analysis

Similar to one of our recent studies reporting on the entire rabbit cohort,[11] we conducted the following analysis. CPP was determined as: MAP – ICP. Systolic flow velocity (FVs) was derived by calculating the maximum of the recorded high frequency TCD maximum flow velocity (FV) envelope over a 0.5 second window, updated every 0.25 seconds. Mean flow velocity (FVm) was calculated using the average of the recorded high frequency TCD maximum FV envelope over a 10 second window, updated every 10 seconds without data overlap. Pulse amplitude of ICP (AMP) was determined by calculating the fundamental Fourier amplitude of the ICP signal over a 10 second window, updated every 10 seconds.

This was done over the frequency range consistent with the rabbits HR (ie. 100 – 400 bpm). Finally, 10 second moving averages (without data overlap) were calculated for all recorded signals: ICP, AMP, ABP (ie. producing MAP), CPP, FVm, FVs, LDF based CBF (LDF-CBF).

The archived signals for all 28 of the animals were retrospectively interrogated and analyzed. Utilizing ICM+ software, plots for LDF versus CPP and FVm/FVs versus CPP were constructed. These were inspected visually for overall trend and the presence of a visible "break point" in LDF/FVm/FVs where future piecewise linear regression analysis would potentially be able to identify an accurate LLA. It was found that only 12 of the animals had sufficient recordings to allow for the accurate assessment of the LLA (given insufficient data after artifact removal to clearly identify a LLA), and thus only 12 animals were utilized for the remainder of the study. The reason for eliminating 16 animals from future analysis stemmed from LDF and/or TCD probe shift throughout the experiments, leading to loss of viable signal and inability to derive an accurate LLA. The apparatus employed for holding the LDF and TCD probes in situ during these experiments in the mid 1990's was inadequate, leading to poor signal acquisition in many animals.

Autoregulation/Cerebrovascular Reactivity Indices

Continuous indices of autoregulation/cerebrovascular reactivity were derived within ICM+ in a similar fashion to other clinical studies.[8,14,15] The following method was conducted for each index, with a summary of these indices found in Table 1. For PRx, we derived a moving Pearson correlation coefficient between ICP and MAP, using 30 consecutive 10 second windows (ie. five minutes of data), updated every 10 seconds. We employed a 10 second update frequency given the relatively short duration of recordings (mean for all animals 28.2 min +/- 8.4 min). Aside from the indices in Table 1, we also derived one index of compensatory reserve, RAP, the correlation between AMP and ICP.

***Table 1 here**

Statistics

All statistical analysis was conducted utilizing R statistical software (R Core Team (2016). R: A language and environment for statistical computing. R Foundation for Statistical Computing, Vienna, Austria. URL https://www.R-project.org/). The following packages were employed: *ggplot2, dplyr, tidyverse, lubridate, segmented, and pROC*. Where significance is reported, alpha was set at 0.05. The following analysis described is identical to that performed by Brady et al.,[9] the only study in existence validating PRx against the LLA. This was done to allow comparison between the results, and potentially provide validation of the results seen within that study.

Finding the LLA

In order to determine the LLA in the 12 animals, we employed piecewise linear regression of either LDF-CBF versus CPP plots, or FVs versus CPP plots. In 3 of the 12 animals, the LDF-CBF signals were not adequate for piecewise regression, and thus FVs versus CPP plots were utilized to find the LLA. The LDF-CBF signal was standardized against the individual animal's baseline LDF-CBF signal, producing "% change of LDF-CBF from baseline". This is similar to other studies evaluating LDF-CBF.[9,11]

The piecewise regression process employed a starting point for estimation of the break-point in either LDF-CBF or FVs. This starting point was visually estimated from the ICM+ plots of LDF-CBF versus CPP or FVs versus CPP, described above. Despite this initial visual inspection, the automated piece-wise linear regression was conducted via the "segmented" computational package within R statistical software. The

"start point" is only a starting reference for the automated algorithm to perform the piecewise regression, with the full range of available CPP values tested during the process. This process functions on the assumption of continuity in data, splitting the data into two distinct linear segments. The intersection point of these two linear segments is considered the breakpoint in the piecewise function. The breakpoint identified by the piecewise regression process is one which minimized the sum residual square error (SSE) of the two linear segments, above and below this point. This breakpoint represents the LLA, with this method being described previously for the determination of the LLA in experimental models.[9] This was conducted for each animal, with piecewise regression plots produced denoting the 95% confidence interval (CI) for each fitted linear segment. Finally, the mean LLA for the cohort of 12 rabbits was determined by averaging all 12 LLA values obtained.

Finding the "Cushing's Response Point"

Given this animal model involved sustained intra-cranial hypertension, the profound sympathetic surge seen during herniation could influence the relationship between MAP and ICP or AMP, leading to overwhelming positive trends in PRx, PAx and RAC below the LLA. Thus, we wanted to see if there was a difference between the LLA and when the Cushing's response[16] was seen. We performed separate piecewise linear regression analysis of MAP versus CPP plots, looking for a break point where as CPP continues to decrease, we see a dramatic increase in MAP, corresponding the point where the Cushing's response takes effect. The breakpoint identified by the piecewise regression process is one which minimized the SSE of the two linear segments, above and below this point. This was conducted for each animal, with piecewise regression plots produced denoting the 95% CI for each fitted linear segment. Finally, the mean "Cushing's Point" for the cohort of 12 rabbits was determined by averaging all 12

breakpoint values of MAP versus CPP. The mean LLA was compared to the mean "Cushing's Point" via student t-test, to assess statistical significance.

Binned Cohort Data and Plot

After delineating the mean LLA for the cohort, we then produced cohort wide plots to inspect the population trend of various physiologic measures against the LLA. We first binned all data across 2.5 mm Hg bins of CPP, using R statistical software. The following error bar plots were then produced: LDF-CBF vs. CPP, FVs vs. CPP, PRx vs. CPP, PAx vs. CPP, AMP vs. CPP, and Lx vs. CPP. All other indices described above in Table 1 were explored, but failed to produce conclusive results within this model of intra-cranial hypertension to either confirm or refute their association with the LLA. Thus, these plots were not reported within the body of this manuscript, but can be found in the supplementary materials.

Comparing CPP for Various Clinical Thresholds of PRx and PAx to LLA

We wished to conduct a rough comparison of CPP for clinically defined thresholds of PRx and PAx to CPP at the LLA, defined via piecewise regression in each animal. To do so, we employed a simplified piecewise linear regression of PRx vs. CPP and PAx vs. CPP, using these models to determine CPP in each animal for the following thresholds of PRx[16] and PAx defined in TBI patients. For PRx, the thresholds of 0, +0.25 and +0.35 were tested, based on previous work in TBI[16] and currently unpublished data from our lab. For PAx, the thresholds of 0 and +0.25 were tested, based on unpublished work from our lab. We then compared the CPP values at each threshold for PRx and PAx, with the CPP values at the LLA, using a Bland-Altman analysis. The Bland-Altman analysis was only conducted for those index thresholds which displayed statistically significant Pearson correlation coefficients with the LLA.

Prediction of Continuous Indices for Impaired Autoregulation

As done in Brady et al.,[9] we performed receiver operating curve (ROC) analysis of PRx, PAx and Lx across the cohort defined LLA. This was conducted in order to determine the ability of these indices to predict being either above or below the LLA. For each rabbit, 1 mean value for each variable was obtained at each 2.5 mm Hg bin of CPP (ie. CPP = 40 mm Hg, 42.5 mm Hg, etc.). We utilized 2.5 mm Hg bins of CPP for the ROC analysis, to provide improved ROC prediction compared to the 5 mm Hg binned data utilized within the previous study by Brady et al.[9]

This data was then given the binary designation of being above the LLA, or below the LLA, based on the LLA defined previously. The data from all 12 rabbits was then utilized for the ROC analysis. Area under the curve (AUC) for the ROC's was reported and 95% CI reported via Delong method. Significance values (ie. p-values) for the AUC's were derived from univariate logistic regression analysis. Comparison between AUC's was conducted utilizing Delong's test.

Results:

Defining the LLA

Piecewise linear regression was conducted in each rabbit. Nine of the rabbits had this analysis conducted on the LDF-CBF vs. CPP plots, while in 3 animals it was conducted on the FVs vs. CPP plots.

Across all rabbits, the mean LLA was determined to be 51.5 +/- 8.2 mm Hg. Figure 1 displays the piecewise linear regression for two animals, with their corresponding scatter plots. Panel A displays an example of the plots for ICP, MAP, CPP, LDF and FVs over time during the experiment. Panel B and C denote an example of piecewise regression using the LDF-CBF vs. CPP plot, and Panel D and E denote the same using the FVs vs. CPP plot. Figure 2, displays the % Change in LDF-CBF vs. CPP error bar plot for the entire rabbit cohort, demonstrating a dramatic drop in LDF signal below the defined LLA (ie. ~50 mm Hg). All piecewise regression of % Change in LDF-CBF versus CPP and FVs versus CPP, with scatter plots, for each animal can be seen in Appendix A of the supplementary materials.

Defining the "Cushing's Point"

Piecewise linear regression of MAP versus CPP was conducted for each rabbit. Across all rabbits the mean "Cushing's Point", where with further decrease in CPP we saw dramatic increases in MAP, was 42.4 +/- 9.8 mm Hg. Figure 3 displays an example of the piecewise regression between CPP and MAP, identifying the "Cushing's Point". Comparing the LLA and the Cushing's point across all animals, via the student's t-test, the LLA and Cushing's point were noted to be statistically different ($t=2.396$, $p=0.027$).

*Figure 1 here

*Figure 2 here

*Figure 3 here

Autoregulation/Cerebrovascular Reactivity across the LLA

We produced various cohort-wide plots of continuous indices of autoregulation/cerebrovascular reactivity across the LLA, as defined above. Figure 4 displays PRx and PAx error bar plots against binned CPP. It can be seen that, as reported in Brady et al.,[9] PRx correlates with the LLA, becoming progressively more positive (denoting "impaired" autoregulation) below the LLA of ~50 mm Hg (Panel A). Similarly, we are able to demonstrate the PAx also correlates with the LLA within this model (Panel B). Finally, given the LLA was mainly defined using LDF-CBF signal across a range of CPP, the LDF derived continuous index of autoregulation (Lx) also correlated with the LLA (Appendix B). Of note for all of the above relationships, these trends can be seen between the LLA (vertical dashed line) and the Cushing's point (vertical solid line), indicating that these relationships to the LLA are seen before the Cushing's response develops.

All other indices described within the methods section were explored (ie. Table 1), but failed to produce conclusive results within this model of intra-cranial hypertension to either confirm or refute their association with the LLA. Thus, these plots were not reported within the body of this manuscript, but can be found within the supplementary materials.

*Figure 4 here

Comparing CPP for Various Clinical Thresholds of PRx and PAx to LLA

For each animal, the CPP at each threshold for PRx and PAx was roughly derived through a simplified piecewise linear model of PRx vs. CPP and PAx vs. CPP in each individual animal. These CPP values were compared to the CPP for the LLA derived in each animal, as described above. They were compared via Pearson correlation coefficient. Table 2 displays these results. RAC, Sx and Mx were not interrogated given their poor performance in the above analysis and inability to produce reliable piecewise models for RAC vs CPP, Sx vs CPP and Mx vs. CPP.

**Table 2 here*

The Pearson correlation between the CPP values at a PRx threshold of +0.35, with the CPP at the LLA, demonstrates that this clinical threshold may represent the LLA, though this isn't definitive. Similarly, the Pearson correlation between the CPP values at PAx thresholds of 0 and +0.25, with the CPP at the LLA, demonstrate that theses clinical threshold may also represent the LLA. Bland-Altman analysis for the 3 statistically significant index thresholds (ie. PRx +0.35, PAx 0, and PAx +0.25) demonstrated poor agreement with bias, when comparing the CPP at each index thresholds to the CPP at the LLA. All Bland-Altman analysis and plots can be found in Appendix C of the supplementary materials.

LLA ROC Analysis

All ROC curves for PRx, PAx and Lx can be seen within Appendix D of the supplementary materials. Through ROC analysis across the LLA, using the data from the 12 rabbits, we were able to identify the AUC's for each continuous index. The AUC for PRx, PAx and RAC was: 0.795 (95% CI: 0.731 – 0.857, p<0.0001), 0.703 (95% CI: 0.631 – 0.775, p<0.0001), and 0.558 (95% CI: 0.478 – 0.637, p=0.325), respectively. Finally, the AUC for Lx was 0.740 (95% CI: 0.668 – 0.812, p<0.0001). Comparing AUC's via Delong's test, there was no significant difference between the AUC generated for PRx, PAx and Lx (all p>0.05).

Discussion:

Through retrospective analysis of this experimental model data, we have been able to provide validation for the previously described claims that PRx respects the LLA.[9] In our above described study, we have been able to reproduce all of these results in a white NZ rabbit model of intra-cranial hypertension, which has not been described previously. Thus, we have provided further evidence to support the use of PRx in monitoring autoregulatory capacity, only the second study to do so. This is the only study to do so during intra-cranial hypertension, a clinically relevant physiologic process in for monitoring PRx in TBI. Finally, we were also able to roughly evaluate the CPP at various clinically relevant thresholds of PRx, defined in TBI patients. Interestingly, we were able to provide some preliminary results to support that the PRx threshold of +0.35 may correlate with the LLA within this model of intra-cranial hypertension, though agreement on Bland-Altman was poor.

Furthermore, we have been able to provide validating evidence to support that the ICP index PAx, also correlates with the LLA, allowing for confidence in its application as a measure of autoregulatory capacity/cerebrovascular reactivity. This has never been described previously for this index. In addition,

similar to PRx, we were also able to provide some preliminary results to support that the clinically relevant PAx thresholds of 0 and +0.25 may correlate with the LLA within this model of intra-cranial hypertension, via a rough assessment through Pearson's correlation coefficients between the CPP at the LLA and that at the corresponding PAx thresholds. However, importantly, the agreement on Bland-Altman analysis was poor.

Of additional interest, the ICP derived index RAC failed to demonstrate any reliable evidence that it correlated with the LLA within this model of sustained intra-cranial hypertension, where the other ICP derived indices performed well. RAC is derived from the correlation between AMP and CPP. During this intra-cranial hypertension experiment, AMP was constantly increasing, with CPP decreasing secondary to elevated ICP (ie. not a drop in MAP). Thus, the correlation derived between AMP and CPP during such a physiologic event will be negative in nature. This was seen in the persistently negative values for RAC derived in every animal. Thus, it isn't that surprising that we failed to see a dramatic response in RAC below the LLA. It may be that the failure of RAC to display a significant relationship to the LLA is a function of the particular model used, not the index. There exists a potential for a model of isolated arterial hypotension, leading to decreased CPP, to display a different trend in RAC across the LLA. This will be explored in Part II of this manuscript series. Furthermore, an upper break-point in AMP was not seen in this subpopulation of rabbits (n=12), as has been described in other animal[11] and clinical studies.[18] This is likely secondary to the Cushing's sympathetic response seen within the animals during this experiment, which has been previously described.[11] This Cushing's response led to a preservation of, and increase in, MAP during elevation of ICP.[11] It is possible that if this break-point in AMP were observed (See Appendix E of the supplementary materials), after which AMP would precipitously drop, it would lead to a rapid rise in RAC to more positive values. Whether or not this potential physiologic event would have led to RAC correlating with the LLA is unknown, and requires further investigation.

Another finding of interest is the gap between PRx at the LLA (ie. ~+0.30 from Figure 4A), and a negative PRx value, commonly associated with "intact" autoregulation. This difference between what we clinically attribute to the threshold for "impaired" vascular reactivity (ie. zero) and the LLA seen within this animal model is unknown. Thus, further research is required to determine what physiologic relevance the PRx threshold of zero represents, as it appears to not represent the LLA.

Furthermore, the LLA marked on the figures in this study is the mean LLA for the entire cohort of animals. This is important to recognize, as in humans the LLA likely varies significantly from patient to patient secondary to pre-morbid status and physiologic insults suffered during the course of illness, providing the rationale behind investigations into CPP optimum as a therapeutic target in TBI.

Finally, through the use of linear piecewise regression of CPP versus MAP, we were able to identify the point at which the sympathetic driven Cushing's response occurred, at a mean CPP of 42.4 +/- 9.8 mm Hg. This point was statistically different from the mean LLA of 51.5 +/-8.2 mm Hg ($p=0.027$). Thus, between the LLA and the Cushing's point, the ICP and TCD derived indices were uninfluenced by the sympathetic response seen during a Cushing's response. Hence, the trend towards progressively more positive index values seen for PRx and PAx, confirms that these indices respect the LLA.

Limitations

Despite the interesting results found within this study, there are some important limitations which should be highlighted. First, this study is a retrospective assessment of archived experimental data. In addition, the model focuses on rabbits, which limits the translation of results to clinical monitoring in humans. However, the rabbit cerebral circulation behaves in a similar manner, in terms of reactivity to changes in MAP and pCO_2, leading to its use in various experiments regarding vascular reactivity over

the preceding decades.[19,20] Thus, the response of the rabbits cerebral vascular system does carry some parallels to that of humans, though it must be acknowledged it is not identical.[20]

Second, out of the 28 rabbits included in the original experiment, only 12 had sufficient quality archived signals for defining and interrogating the LLA, related to issues with the technique of signal acquisition for LDF and TCD, eluded to within the methods section. In addition, the model consisted of an isolated basilar artery fed circulation. This was done in order to allow for a global assessment of CBFV via TCD. This exact model hasn't been validated. There does exist potential for dilation of the basilar as a result of the isolated circulation. However, given the FVs versus CPP and LDF versus CPP produced similar relationships as CPP was decreased towards the LLA, we feel that the results derived from TCD are valid.

Third, despite "controlling" the pCO_2 throughout the experiment, the standard deviation of 5.7 mm Hg could still have impacted the vasoreactivity within the animal models. This should be acknowledged as a limitation.

Fourth, this model only employed sustained intra-cranial pressure as a driver of CPP reduction. There were no animals studied with arterial hypotension in isolation (ie. with normal ICP). Extreme ICP elevation as a driver of CPP reduction has not been explored fully in the past, as most of the literature for PRx, both experimental and clinical, focuses on PRx as a measure of vascular reactivity during fluctuations in CPP, predominantly secondary to changes in MAP. This concept of using PRx to estimate cerebral autoregulation during MAP fluctuations has led to an expansive literature on PRx in TBI, and the concept behind CPP optimum. However, aside from fluctuations in MAP driving CPP changes, elevated ICP is another important driver of CPP change during acute brain injury. Thus, evaluating PRx during elevated ICP is crucial to our understanding of the wide spread clinical applicability of PRx monitoring, especially in TBI patients. This makes the results of this study important for future application of this monitoring in TBI patients. However, the results of this study must be taken with caution, given we can

only comment on the relationship between these continuous indices and the LLA during extreme ICP increases. Part II of this manuscript series will focus on a piglet model of pure arterial hypotension, in order to explore the ICP derived indices and the LLA during this physiologic event.

Fifth, the other indices derived from ICP and TCD (RAC, Mx and Sx), described within the methods section, failed to produce reliable data within this model of intra-cranial hypertension to either confirm or refute their association with the LLA. The error bar plots and ROC analysis for RAC and the TCD indices can be found within the supplementary materials, Appendix F. Given the poor performance of these indices (ie. RAC, and TCD based indices), it is unknown as to whether they can measure the LLA during sustained intra-cranial hypertension. Thus, they were not reported further within the body of the manuscript, and we elected to focus just on PRx and PAx. This particular model of intra-cranial hypertension may be why the other indices tested (RAC, Sx and Mx) failed to produce reliable data to confirm or refute their association with the LLA.

Sixth, the rate of rise in ICP was fairly rapid within this model (ie. ~30 min), this may have played a part in the relatively noisy data and fluctuations seen within the error bar plots provided. It is unknown if a longer period of rise in ICP would have led to "cleaner" data, and the ability to provide validation for the other indices. There is much further work required to confirm these results during other physiologic conditions.

Seventh, despite providing validating and confirmatory evidence for the use of PRx and PAx for monitoring the LLA, this study does not address the upper limit of autoregulation (ULA). Again, further studies are required to address whether these indices also respect the ULA.

Eighth, the use of PRx to derive patient specific optimal CPP targets deserves mention. CPP optimum can be derived by plotting PRx versus CPP, evaluating the minimum of the parabolic relationship as the optimal CPP for a given patient (corresponding to the lowest PRx value, and thus the "best"

autoregulatory state). To date, various studies have linked the time spent outside of CPP optimum and worse patient global outcome in adult TBI.[21] This concept relies on some degree of preserved autoregulatory capacity, which may not be the case during extreme injury. Without vascular reactivity, any changes in MAP or CPP lead to direct pressure passivity in ICP, abolishing the ability to determine a CPP optimum. This can be the case during extreme ICP elevations in TBI. However, the results of this study demonstrate that within experimental modal of extreme intra-cranial hypertension, PRx does maintain the ability to measure autoregulatory capacity. It is currently unknown if this is the case in humans.

Finally, even though the CPP at some of the clinically defined thresholds for PRx and PAx appeared to be related to the LLA within this rabbit model via Pearson correlation coefficient, one must interpret this with caution. The Bland-Altman analysis indicated poor agreement between the CPP at the LLA and that at all index thresholds tested. Thus, it appears that these index thresholds do not adequately measure the LLA, but may measure some other physiologic event (not yet clearly identified) which is linked to outcome in TBI. As the LLA represents the point at which cerebral autoregulation becomes impaired (ie. not the point at which vascular reactivity is completely lost), the lack of strong associations with CPP at thresholds defined by clinical outcome is not surprising. These thresholds for the ICP defined indices were derived from TBI patient outcome at 6 months post injury. As a result, these index thresholds may represent the severe end of the autoregulation spectrum, the point of complete failure of vascular reactivity. Hence, the relationship between the CPP at thresholds and the LLA may not be robust, as they could be representing different aspects of impaired cerebrovascular reactivity. As well, one must assume that there are individual animal-based differences in vascular reactivity, introducing the influence of potential random effects. Much further interrogation of these clinically defined index thresholds is required, with the current analysis providing some preliminary insight.

Conclusions:

We have provided validation for the ICP derived indices, PRx and PAx, against the LLA within this experimental model of intracranial hypertension. Further analysis of these indices, and others, across the LLA within pure arterial hypotension models is required.

Disclosures: FAZ has received salary support for dedicated research time, during which this project was partially completed. Such salary support came from: the Cambridge Commonwealth Trust Scholarship, the Royal College of Surgeons of Canada – Harry S. Morton Travelling Fellowship in Surgery and the University of Manitoba Clinician Investigator Program.

MC and PS have financial interest in a part of licensing fee for ICM+ software (Cambridge Enterprise Ltd, UK).

Acknowledgments:

Many thanks to Mr. S. Haarland, H.K. Richards and S.K. Piechnik for sharing recorded experiments, performed in Division Neurosurgery, University of Cambridge in late 1990s.

This work was made possible through salary support through the Cambridge Commonwealth Trust Scholarship, the Royal College of Surgeons of Canada – Harry S. Morton Travelling Fellowship in Surgery and the University of Manitoba Clinician Investigator Program.

MC & DJK are supported by a grant of the Korea Health Technology R&D Project through the Korea Health Industry Development Institute (KHIDI), funded by the Ministry of Health & Welfare, Republic of Korea (grant number : HI17C1790).

JD is supported by a Woolf Fisher Scholarship (NZ).

References:

1. Zeiler, F.A., Donnelly, J., Calviello, L., Smielewski, P., Menon, D.K., and Czosnyka, M. (2017). Pressure Autoregulation Measurement Techniques in Adult Traumatic Brain Injury, Part II: A Scoping Review of Continuous Methods. J. Neurotrauma 2017 Sep 26. doi: 10.1089/neu.2017.5086. [Epub ahead of print]

2. Czosnyka, M., Smielewski, P., Kirkpatrick, P., Laing, R.J., Menon, D., and Pickard, J.D. (1997). Continuous assessment of the cerebral vasomotor reactivity in head injury. Neurosurgery 41, 11-17.

3. Sorrentino, E., Diedler, J., Kasprowicz, M., Budohoski, K.P., Haubrich, C., Smielewski, P., Outtrim, J.G., Manktelow, A., Hutchinson, P.J., Pickard, J.D., Menon, D.K., and Czosnyka, M, (2012). Critical thresholds for cerebrovascular reactivity after traumatic brain injury. Neurocrit Care 16(2), 258-266.

4. Czosnyka, M., Miller, C.; and Participants in the International Multidisciplinary Consensus Conference on Multimodality Monitoring. (2014). Monitoring of cerebral autoregulation. Neurocrit Care 21 Suppl 2, S95-102.

5. Sorrentino, E., Diedler, J., Kasprowicz, M., Budohoski, K.P., Haubrich, C., Smielewski, P., Outtrim, J.G., Manktelow, A., Hutchinson, P.J., Pickard, J.D., Menon, D.K., and Czosnyka, M, (2012).

Critical thresholds for cerebrovascular reactivity after traumatic brain injury. Neurocrit Care 16(2), 258-266.

6. Sorrentino, E., Budohoski, K.P., Kasprowicz, M., Smielewski, P., Matta, B., Pickard, J.D., and Czosnyka, M. (2011). Critical thresholds for transcranial Doppler indices of cerebral autoregulation in traumatic brain injury. Neurocrit Care 14(2), 188-193.

7. Budohoski, K.P., Reinhard, M., Aries, M.J., Czosnyka, Z., Smielewski, P., Pickard, J.D., Kirkpatrick, P.J., and Czosnyka, M. (2012). Monitoring cerebral autoregulation after head injury. Which component of transcranial Doppler flow velocity is optimal? Neurocrit Care 17(2):211-8

8. Zeiler, F.A., Donnelly, J., Menon, D.k., Smielewski, P., Zweifel, C., Brady, K., and Czosnyka, M. (2017) Continuous Autoregulatory Indices Derived from Multi-modal Monitoring: Each One is Not Like the Other. J. Neurotrauma. Jun 1. doi: 10.1089/neu.2017.5129. [Epub ahead of print]

9. Brady, K.M., Lee, J.K., Kibler, K.K., Easley, R.B., Koehler, R.C., and Shaffner, D.H. (2008). Continuous measurement of autoregulation by spontaneous fluctuations in cerebral perfusion pressure: comparison of 3 methods. Stroke 39, 2531–2537.

10. Lee, J.K., Kibler, K.K., Benni, P.B., Easley, R.B., Czosnyka, M., Smielewski, P., Koehler, R.C., Shaffner, D.H., and Brady, K.M. (2009). Cerebrovascular reactivity measured by near-infrared spectroscopy. Stroke, 40, 1820-1826.

11. Donnelly, J., Czosnyka, M., Harland, S., Varsos, G.V., Cardim, D., Robba, C., Liu, X., Ainslie, P.N., and Smielewski, P. (2017). Cerebral haemodynamics during experimental intracranial hypertension. J. Cereb Blood Flow Metab 37, 694-705.

12. Czosnyka, M., Richards, H., Kirkpatrick, P., and Pickard J. (1994). Assessment of cerebral autoregulation with ultrasound and laser Doppler wave forms--an experimental study in anesthetized rabbits. Neurosurgery 35, 287-292.

13. Kilkenny, C., Browne, W.J., Cuthill, I.C., Emerson, M., and Altman, D.G. (2010). Improving bioscience research reporting: the ARRIVE guidelines for reporting animal research. PLoS Biol 8, e1000412.

14. Zeiler, F.A., Cardim, D., Donnelly, J., Menon, D.K., Czosnyka, M., and Smielewski, P. (2017). Transcranial Doppler Systolic Flow Index and ICP Derived Cerebrovascular Reactivity Indices in TBI. J. Neurotrauma, Sept 2017, In Press.

15. Zeiler, F.A., Donnelly, J., Cardim, D., Menon, D.K., Smielewski, P., and Czosnyka, M. (2017). ICP versus Laser Doppler Cerebrovascular Reactivity Indices to Assess Brain Autoregulatory Capacity. Neurocrit Care, Sept 2017, In Press.

16. Fodstad, H., Kelly, P.J., and Buchfelder, M. (2006). History of the cushing reflex. Neurosurgery 59, 1132-1137.

17. Sorrentino, E., Diedler, J., Kasprowicz, M., Budohoski, K.P., Haubrich, C., Smielewski, P., Outtrim, J.G., Manktelow, A., Hutchinson, P.J., Pickard, J.D., Menon, D.K., and Czosnyka, M, (2012). Critical thresholds for cerebrovascular reactivity after traumatic brain injury. Neurocrit Care 16, 258-266.

18. Czosnyka, M., Guazzo, E., Whitehouse, M., Smielewski, P., Czosnyka, Z., Kirkpatrick, P., Piechnik, S., and Pickard, J.D. (1996). Significance of intracranial pressure waveform analysis after head injury. Acta Neurochir (Wien) 138, 531-541.

19. Russel, R.W. (1971). The reactivity of the pial circulation of the rabbit to hypercapnia and the effect of vascular occlusion. Brain 94, 623-634.

20. Ryman, T., Brandt, L., Andersson, K.E., and Mellergård, P. (1989). Regional and species differences in vascular reactivity to extracellular potassium. Acta Physiol Scand 136, 151-159.

21. Needham, E., McFadyen, C., Newcombe, V., Synnot, A.J., Czosnyka, M., and Menon, D. (2017). Cerebral Perfusion Pressure Targets Individualized to Pressure-Reactivity Index in Moderate to Severe Traumatic Brain Injury: A Systematic Review. J. Neurotrauma 34, 963-970.

Figures:

Figure 1: Examples of Piecewise Linear Regression Analysis

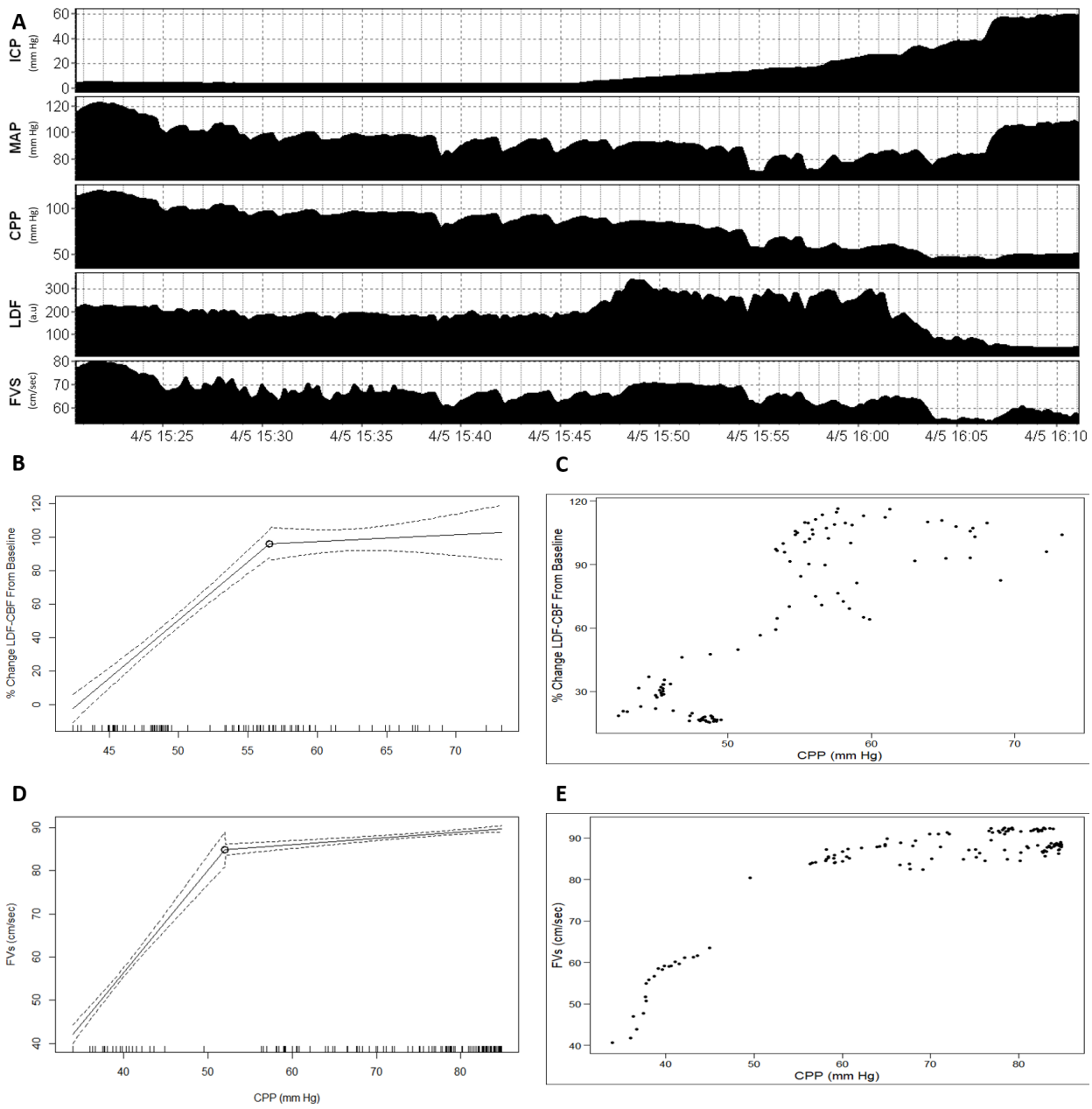

a.u. = arbitrary units, cm = centimeters, CPP = cerebral perfusion pressure, FVs = systolic flow velocity, ICP = intra-cranial pressure, LDF-CBF = laser Doppler flowmetry cerebral blood flow, MAP = mean arterial pressure, mm Hg = millimeters of Mercury, sec = second. Panel A = example of ICP, MAP, CPP, LDF-CBF and FVs over time during the experiment. Pane B = piecewise regression using the LDF-CBF vs. CPP plot, Panel c = scatterplot of LDF-CBF vs. CPP, Panel D = piecewise regression using FVs vs. CPP plot, Panel E = scatterplot of FVs vs. MAP. Note: in piecewise regression plots, the hashed lines along the x-axis denote data point density.

Figure 2: Error Bar Plots – % Change in LDF-CBF vs. CPP – Entire Rabbit Cohort

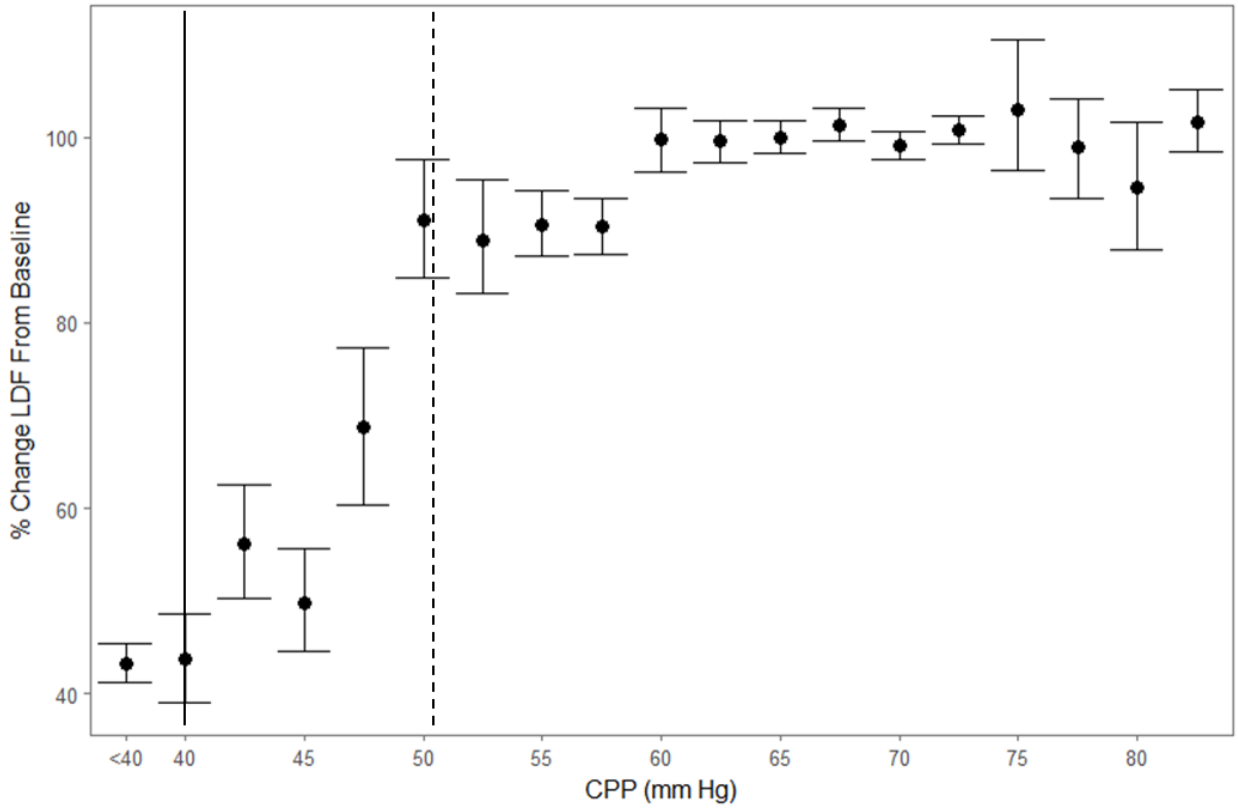

a.u. = arbitrary units, cm = centimeters, CPP = cerebral perfusion pressure, mm Hg = millimeters of Mercury, sec = seconds. Vertical dashed line represents the approximate LLA for the entire cohort. Vertical solid line represents the approximate "Cushing's Point" for the entire cohort.

Figure 3: Piecewise Linear Regression Identifying Cushing's Point – Example

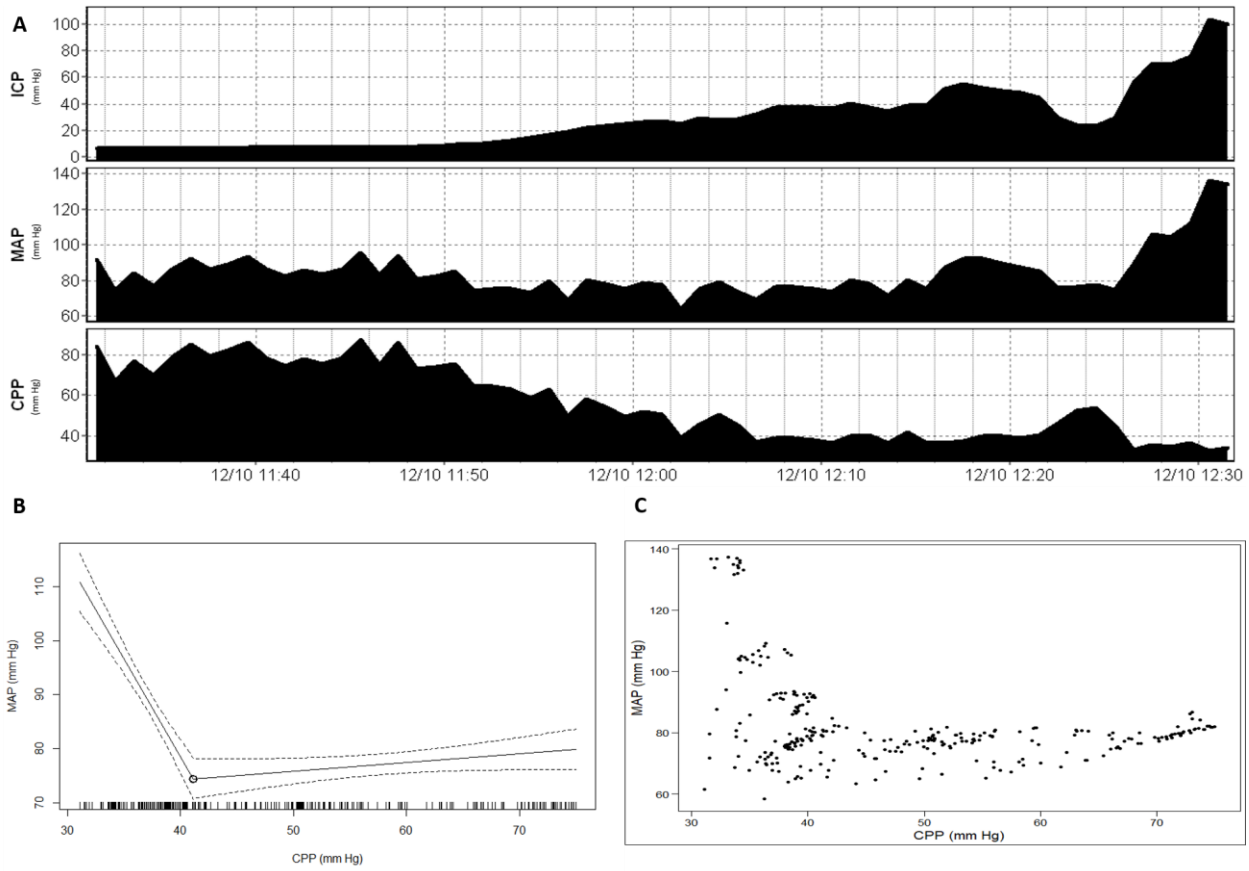

CPP = cerebral perfusion pressure, ICP = intra-cranial pressure, MAP = mean arterial pressure, mm Hg = millimeters of Mercury. Panel A = example of ICP, MAP and CPP over time during the experiment, Panel B = piecewise linear regression of MAP versus CPP, Panel C = scatter plot of MAP versus CPP.

Figure 4: Cohort Based Error Bar Plots of ICP Derived Indices across the LLA

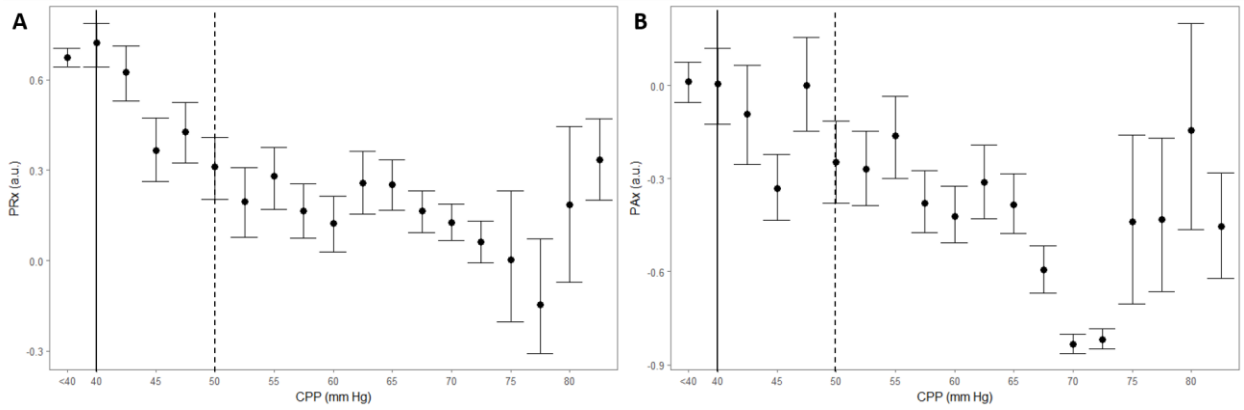

AMP = pulse amplitude of ICP, a.u. = arbitrary units, CPP = cerebral perfusion pressure, LLA = lower limit of autoregulation, MAP = mean arterial pressure, mm Hg = millimeters of Mercury, ICP = intracranial pressure, PAx = pulse amplitude index (correlation between AMP and MAP), PRx = pressure reactivity index (correlation between ICP and MAP). Panel A = PRx versus CPP error bar plot, Panel B = PAx vs. CPP error bar plot. Note: vertical hashed line denotes the approximate LLA, while the vertical solid line represents the approximate Cushing's point.

Table 1: Autoregulation/Cerebrovascular Reactivity Indices and Calculation Methods

Index	Signals Correlated	Signal Averaging (sec)	Pearson Correlation Coefficient Calculation Window (min)	Index Calculation Update Frequency (sec)
PRx	ICP and MAP	10	5	10
PAx	AMP and MAP	10	5	10
RAC	AMP and CPP	10	5	10
Mx	FVm and CPP	10	5	10
Sx	FVs and CPP	10	5	10
Lx	LDF-CBF and MAP	10	5	10

CBF = cerebral blood flow, CPP = cerebral perfusion pressure, FVd = diastolic flow velocity, FVm = mean flow velocity, FVs = systolic flow velocity, ICP = intracranial pressure, LDF-CBF = laser Doppler flowmetry based cerebral blood flow. MAP = mean arterial pressure, min = minute, sec = seconds.

Table 2: Comparison of CPP at Index Threshold to LLA – Pearson Correlation

Index Threshold Tested Against LLA	Pearson Correlation Coefficient with LLA	p-value for Pearson Coefficient
PRx = 0	0.037	0.9121
PRx = +0.25	0.429	0.1881
PRx = +0.35	**0.600**	**0.0507**
PAx = 0	**0.612**	**0.0454**
PAx = +0.25	**0.689**	**0.0190**

AMP = pulse amplitude of ICP, CPP = cerebral perfusion pressure, ICP = intracranial pressure, LLA = lower limit of autoregulation, PAx = pulse amplitude index (correlation between AMP and MAP), PRx = pressure reactivity index (correlation between ICP and MAP). Note: bolded values indicate those which reached statistical significance.

Appendix A: Piecewise Regression and Scatterplots for Each Rabbit

1.

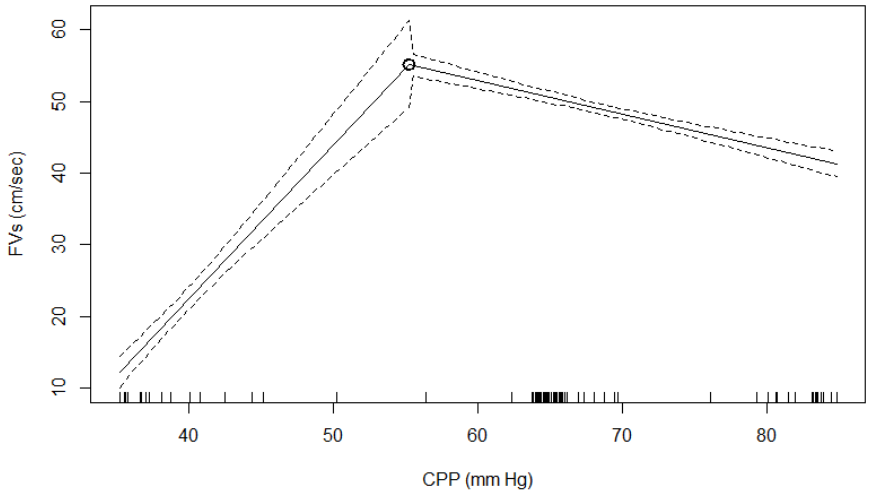

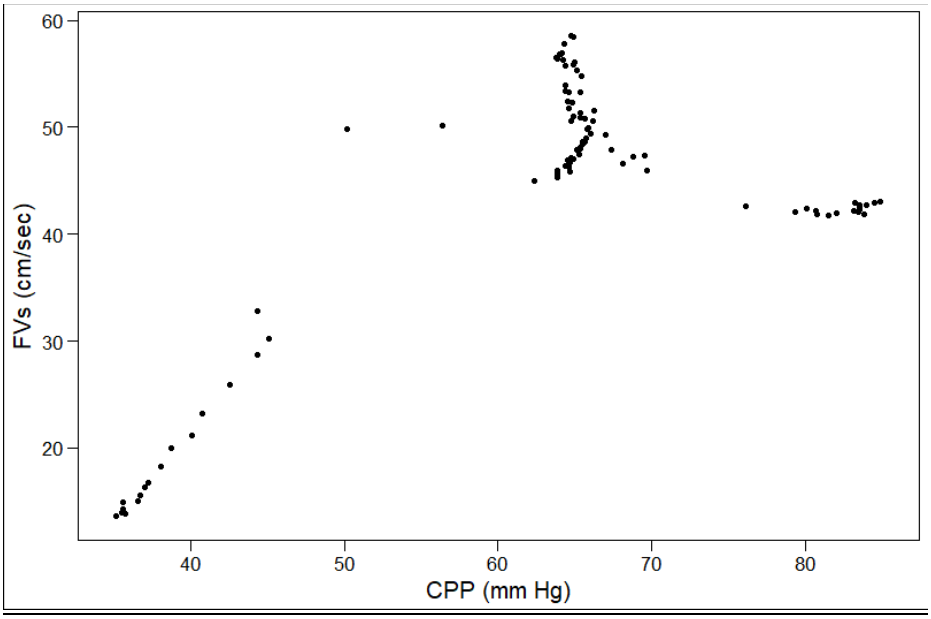

2.

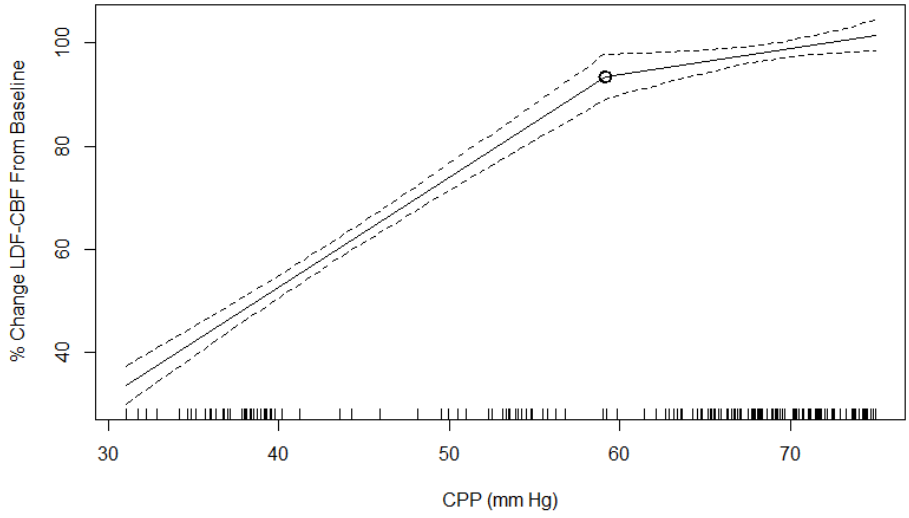
% Change LDF-CBF From Baseline
40
60
80
100
30
40
50
60
70
CPP (mm Hg)

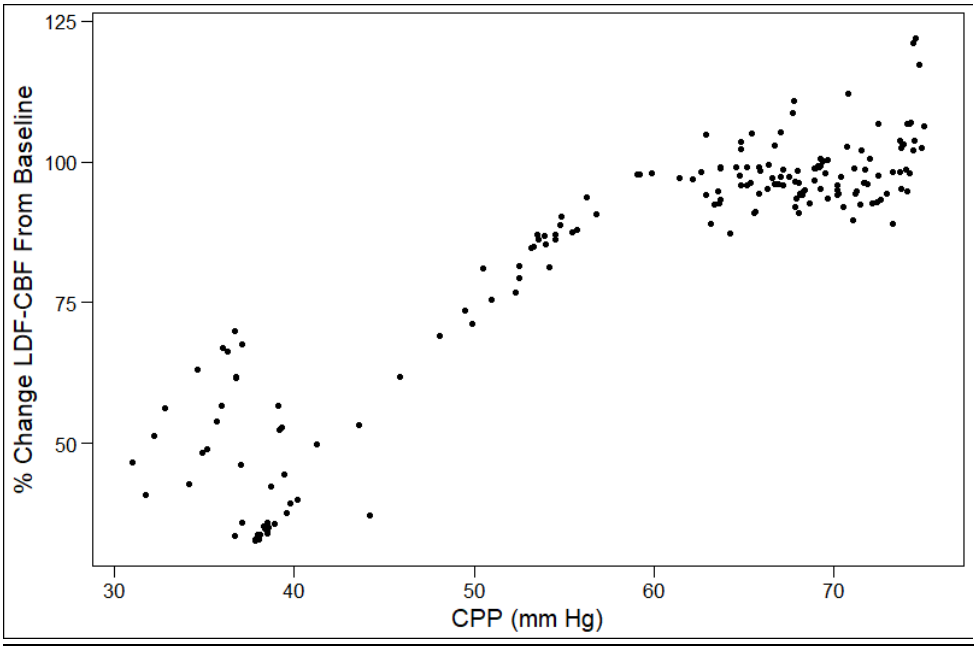
% Change LDF-CBF From Baseline
50
75
100
125
30
40
50
60
70
CPP (mm Hg)

3.

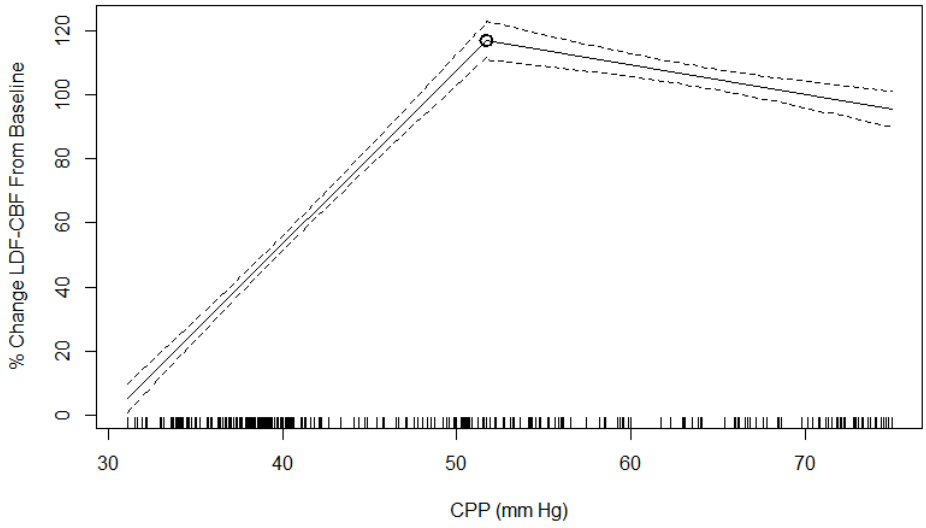
% Change LDF-CBF From Baseline
0
20
40
60
80
100
120
30
40
50
60
70
CPP (mm Hg)

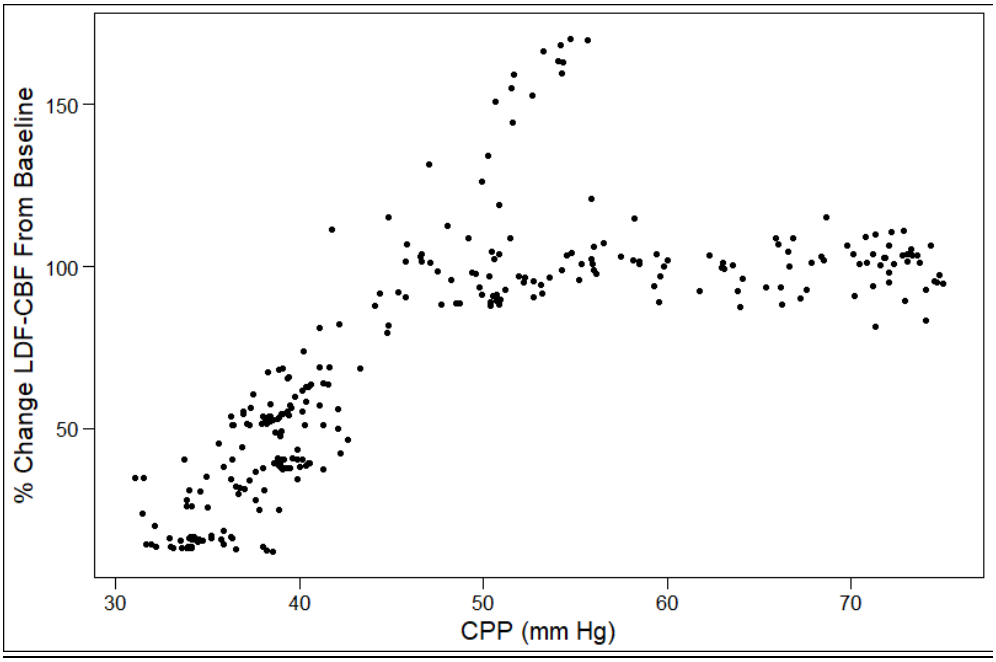
% Change LDF-CBF From Baseline
50
100
150
30
40
50
60
70
CPP (mm Hg)

4.

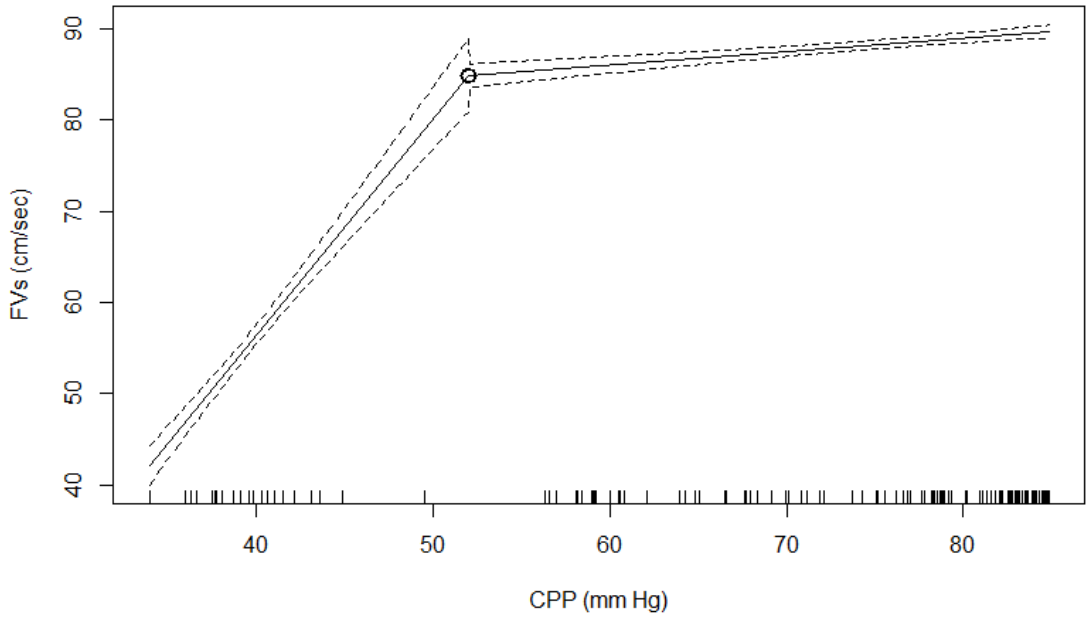
FVs (cm/sec)
90
80
70
60
50
40
40
50
60
70
80
CPP (mm Hg)

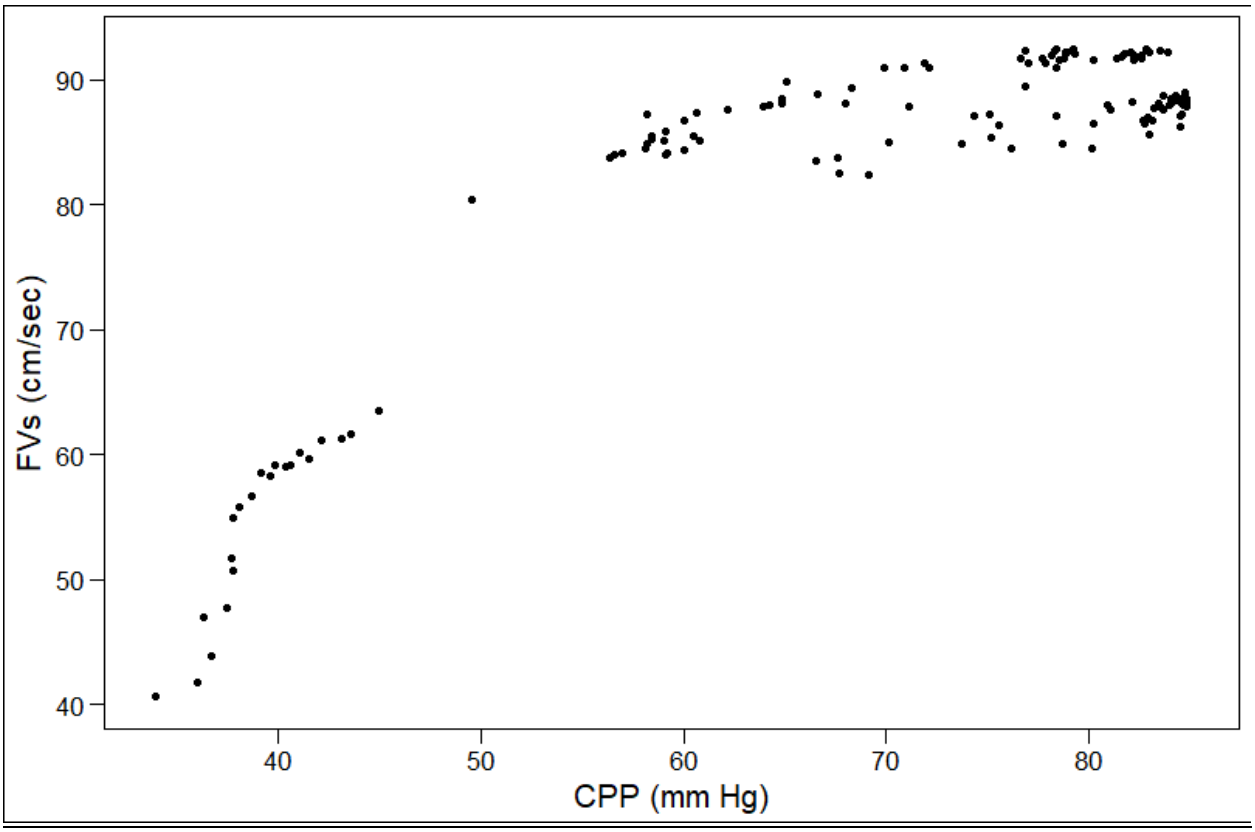
FVs (cm/sec)
90
80
70
60
50
40
40
50
60
70
80
CPP (mm Hg)

5.

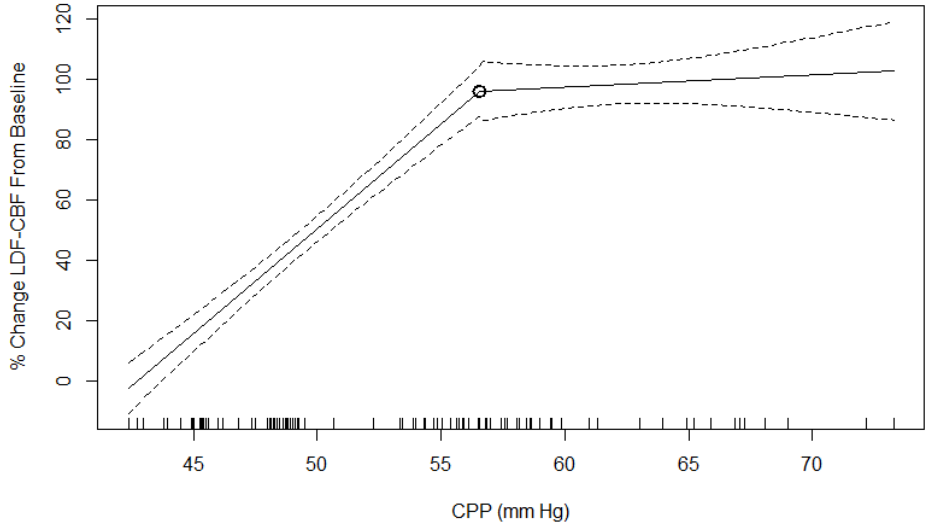
% Change LDF-CBF From Baseline
0
20
40
60
80
100
120
45
50
55
60
65
70
CPP (mm Hg)

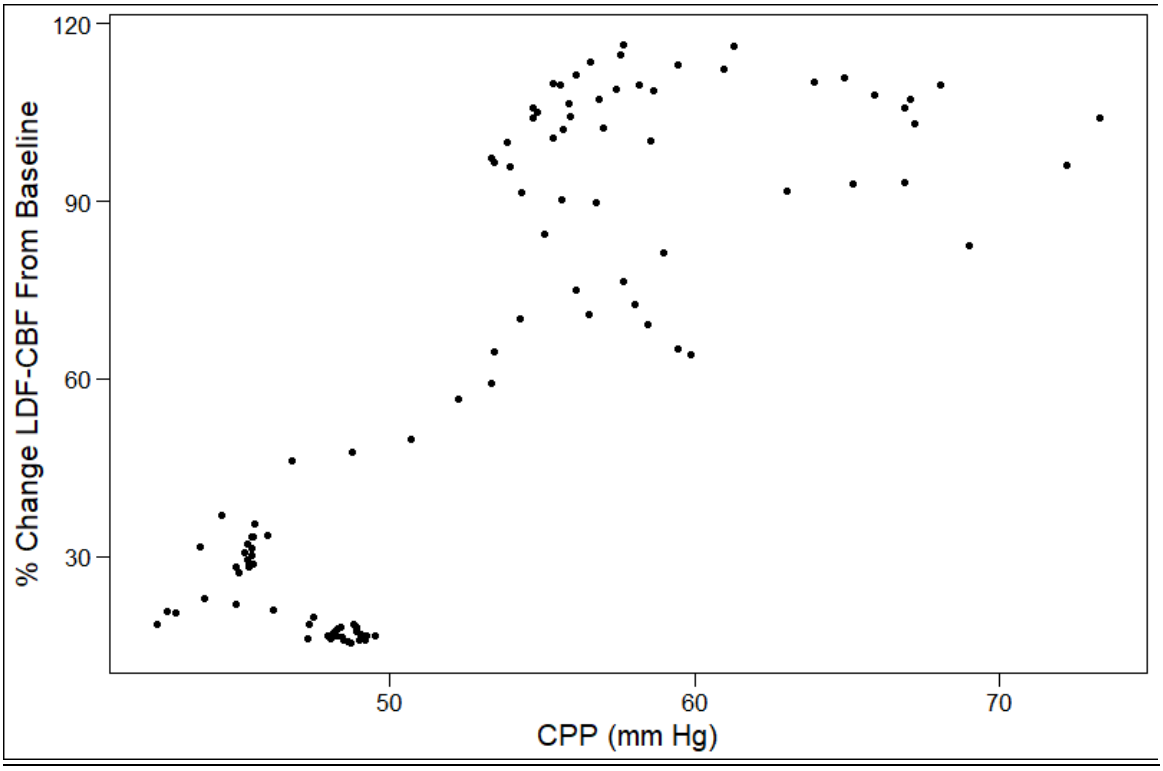
% Change LDF-CBF From Baseline
30
60
90
120
50
60
70
CPP (mm Hg)

6.

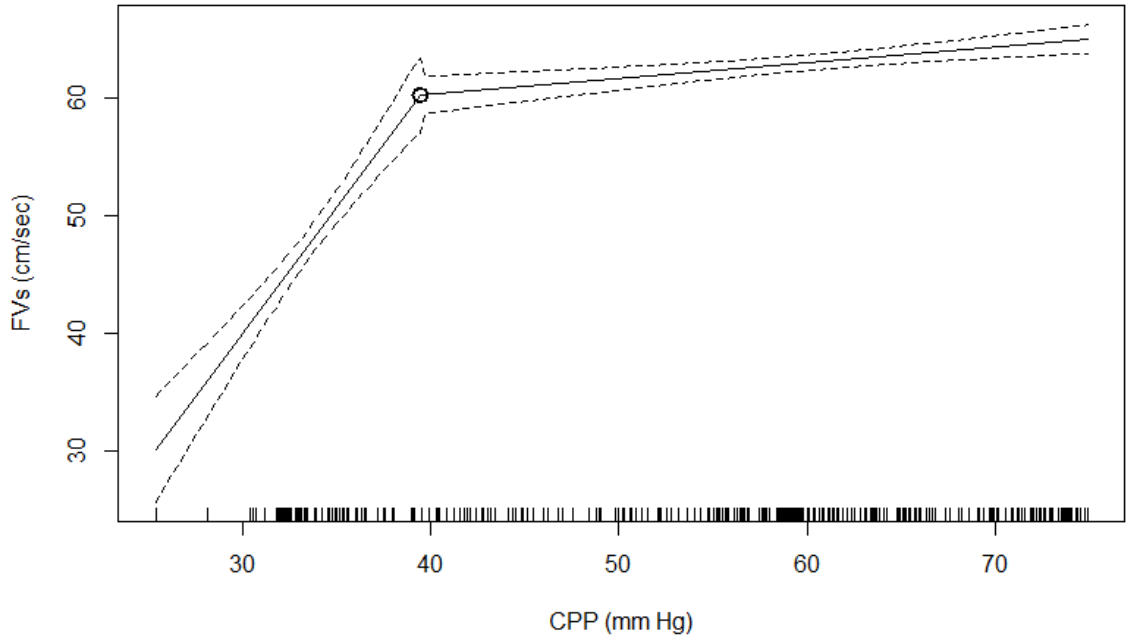
FVs (cm/sec)
30
40
50
60
30
40
50
60
70
CPP (mm Hg)

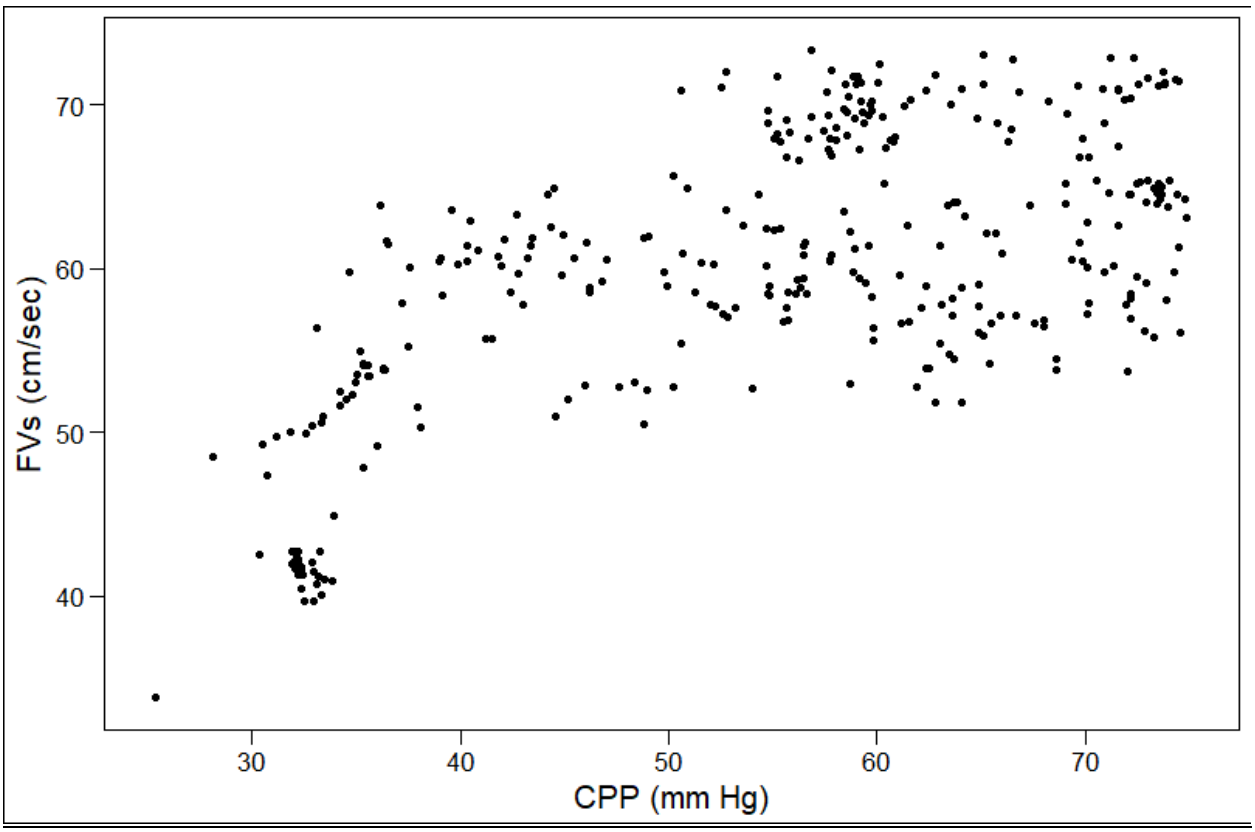
FVs (cm/sec)
40
50
60
70
30
40
50
60
70
CPP (mm Hg)

7.

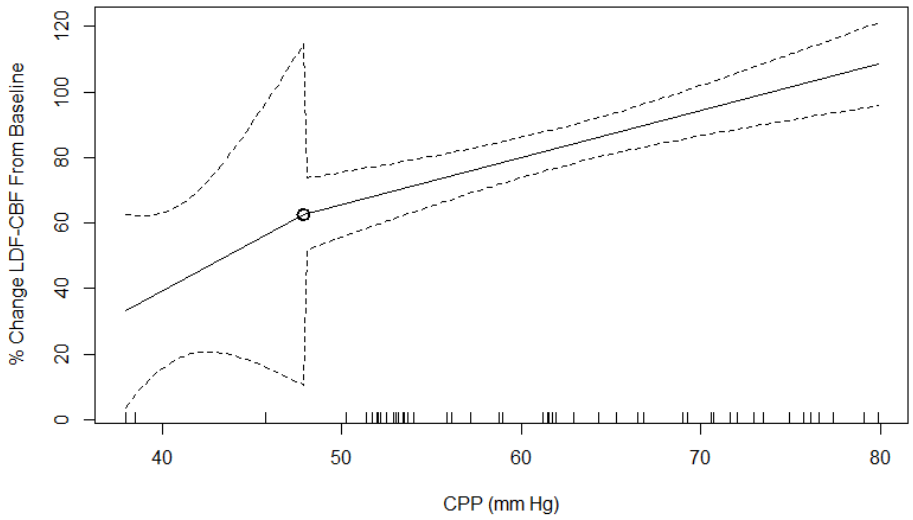
% Change LDF-CBF From Baseline
0
20
40
60
80
100
120
40
50
60
70
80
CPP (mm Hg)

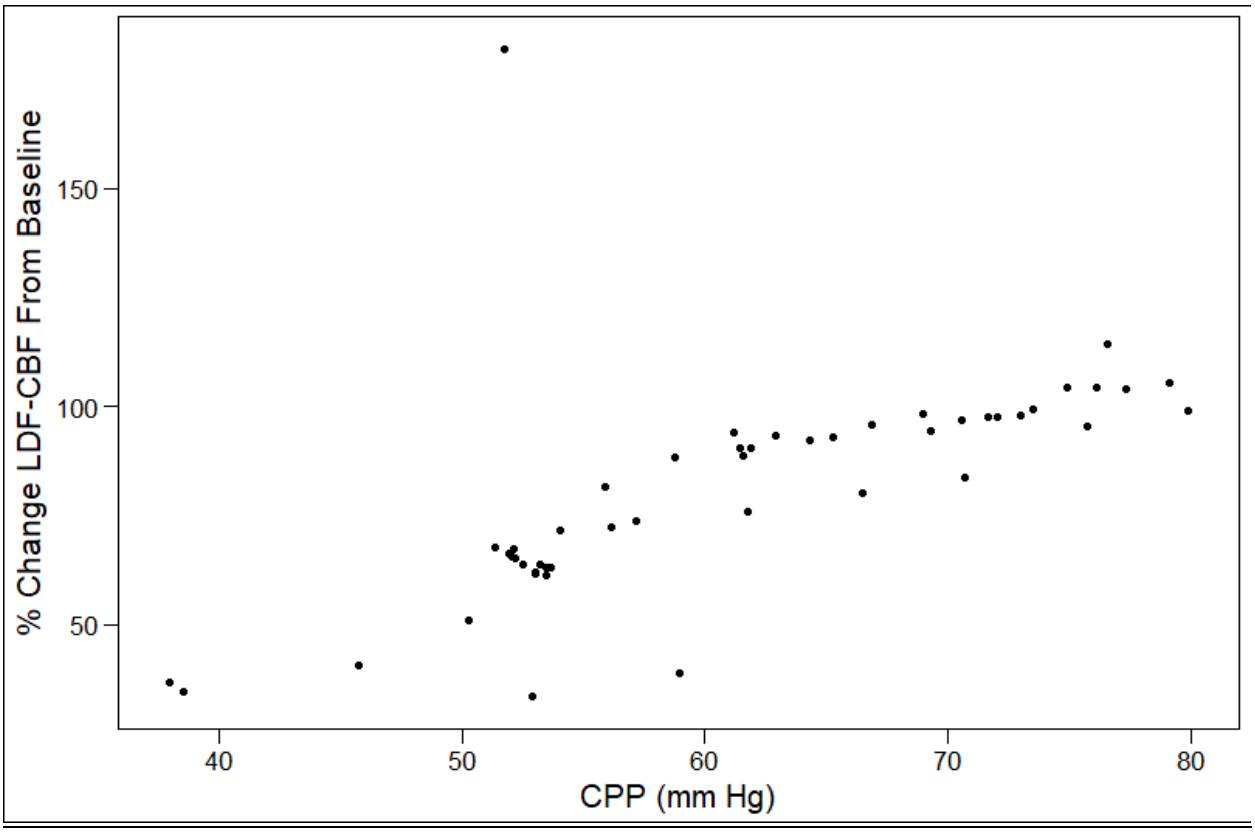
% Change LDF-CBF From Baseline
50
100
150
40
50
60
70
80
CPP (mm Hg)

8.

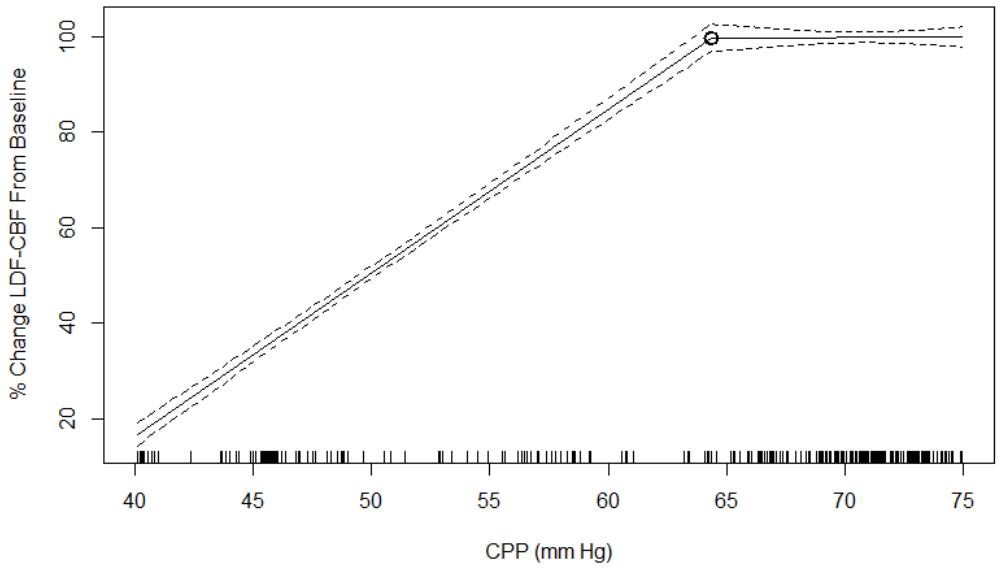
% Change LDF-CBF From Baseline
20
40
60
80
100
40
45
50
55
60
65
70
75
CPP (mm Hg)

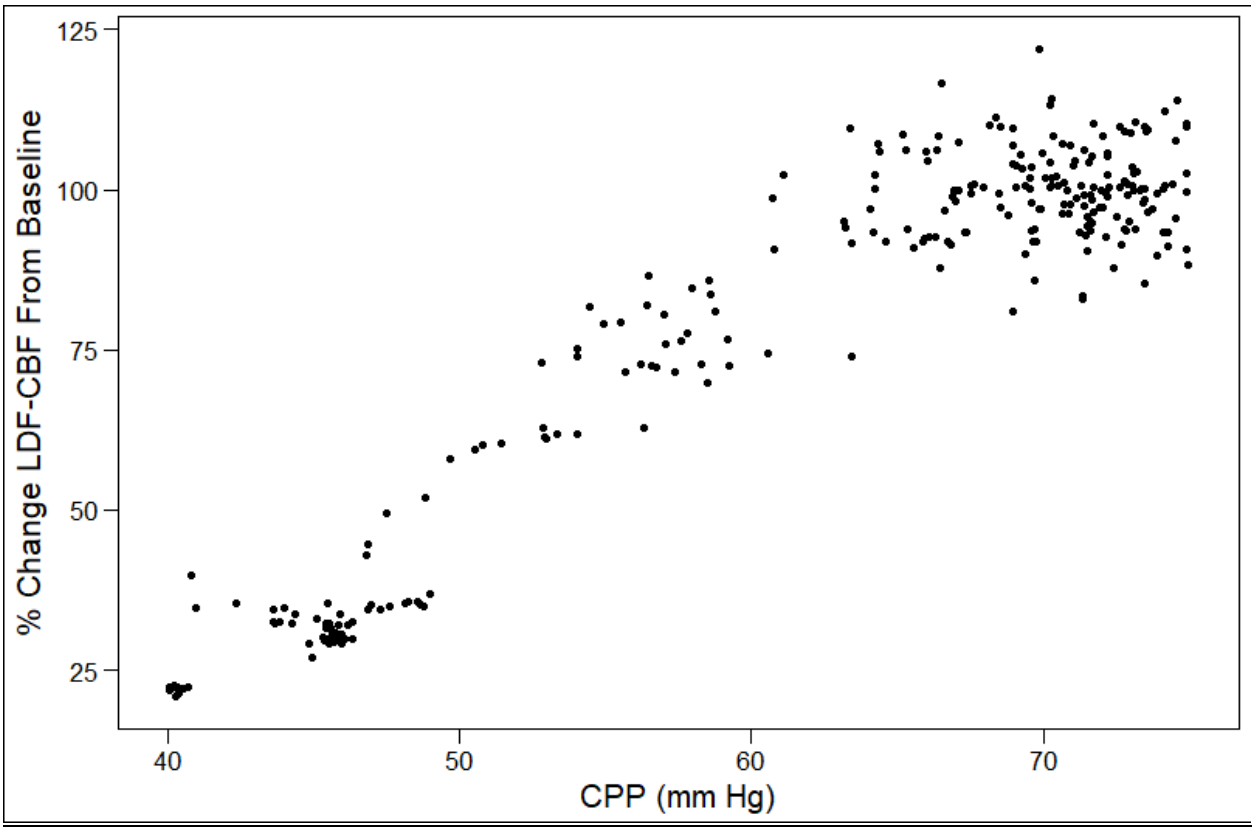
% Change LDF-CBF From Baseline
25
50
75
100
125
40
50
60
70
CPP (mm Hg)

9.

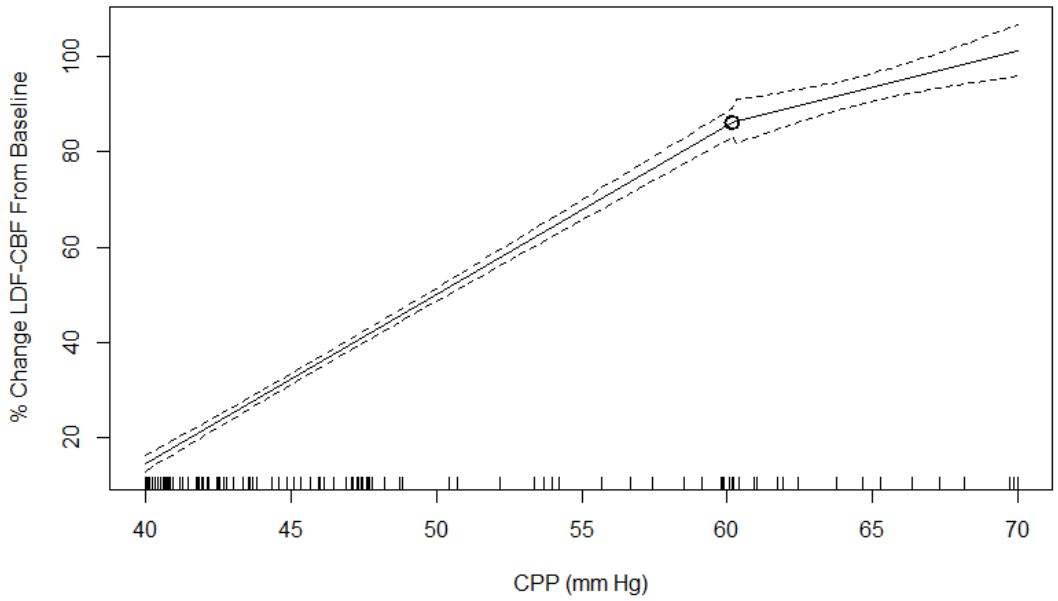
% Change LDF-CBF From Baseline
20
40
60
80
100
40
45
50
55
60
65
70
CPP (mm Hg)

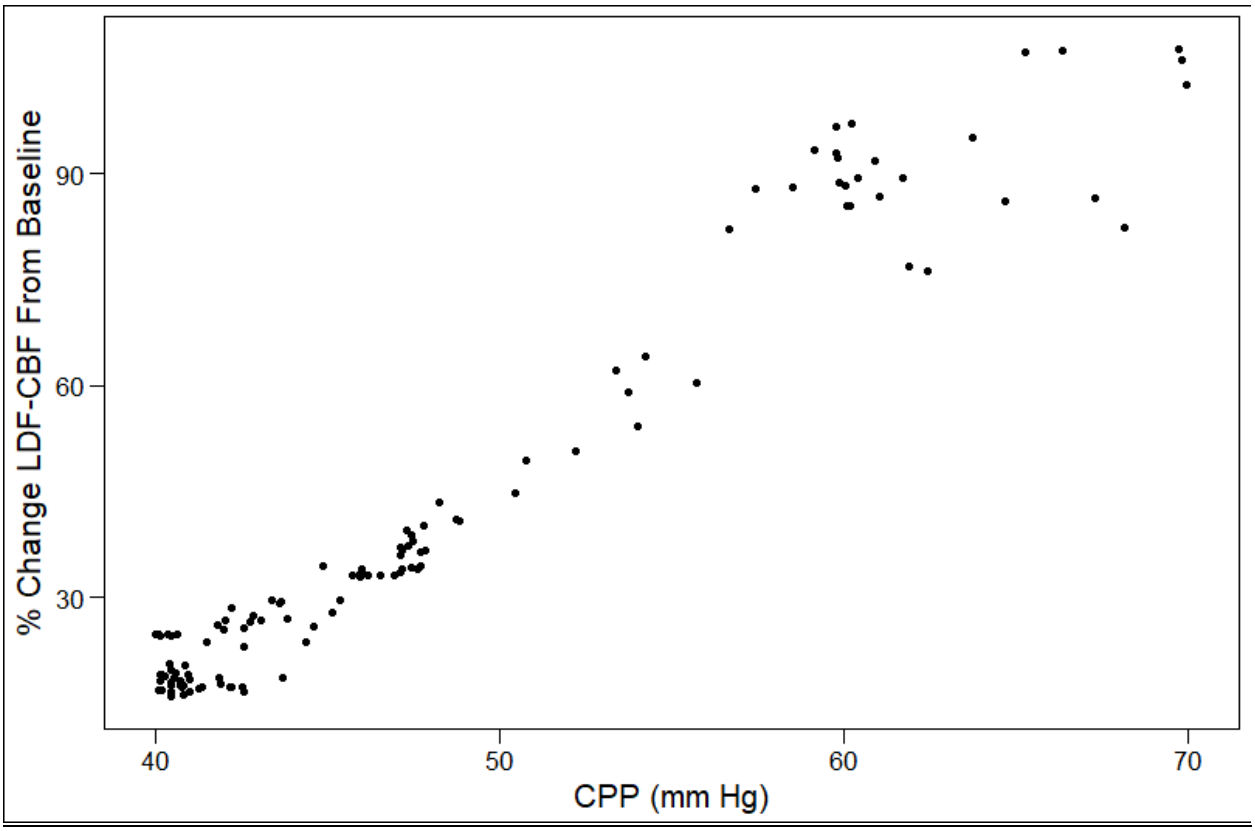
% Change LDF-CBF From Baseline
30
60
90
40
50
60
70
CPP (mm Hg)

10.

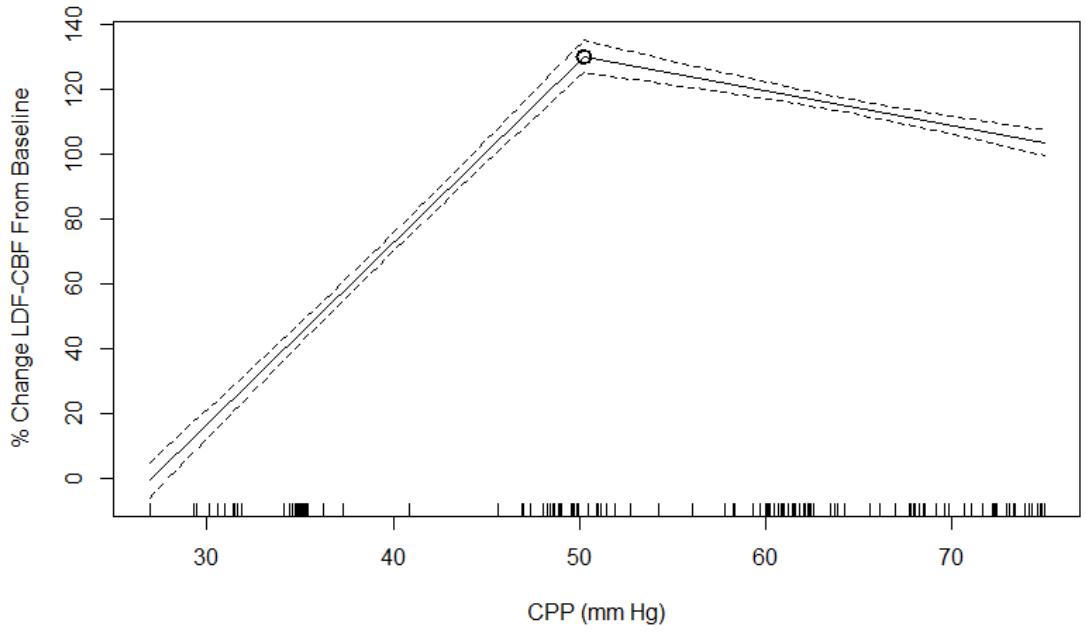
% Change LDF-CBF From Baseline
0
20
40
60
80
100
120
140
30
40
50
60
70
CPP (mm Hg)

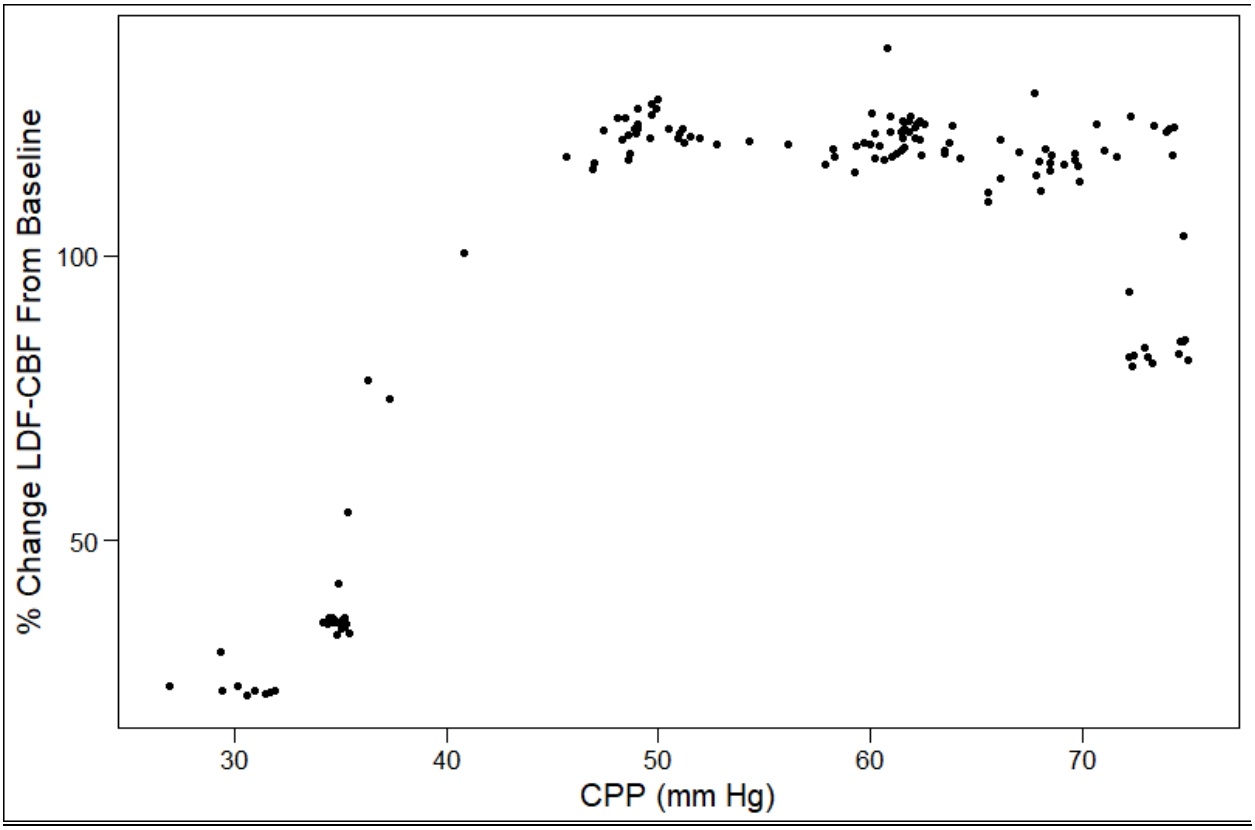
% Change LDF-CBF From Baseline
50
100
30
40
50
60
70
CPP (mm Hg)

11.

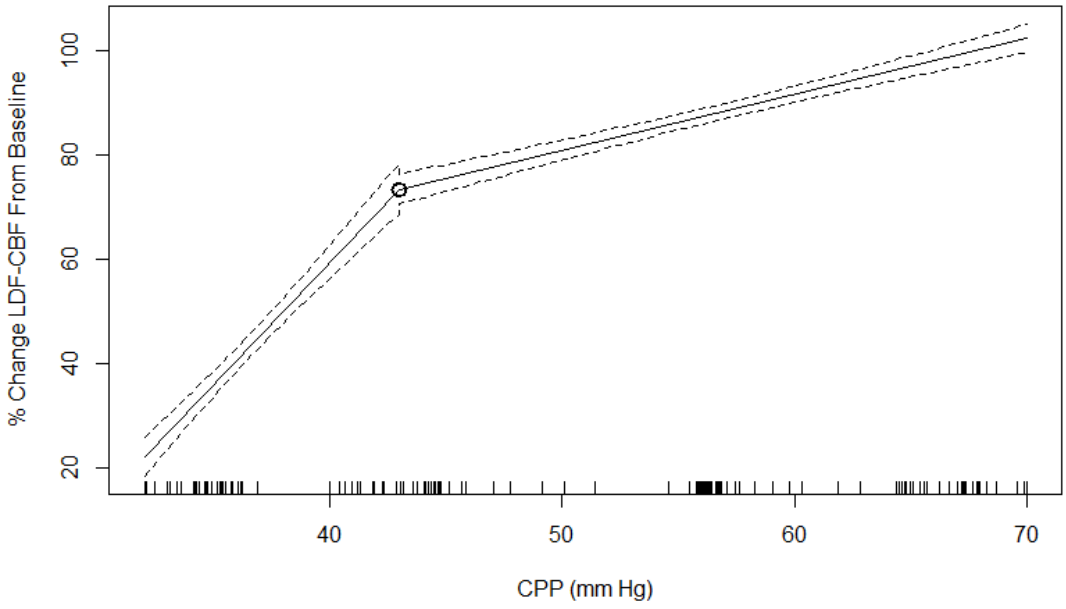
% Change LDF-CBF From Baseline
20
40
60
80
100
40
50
60
70
CPP (mm Hg)

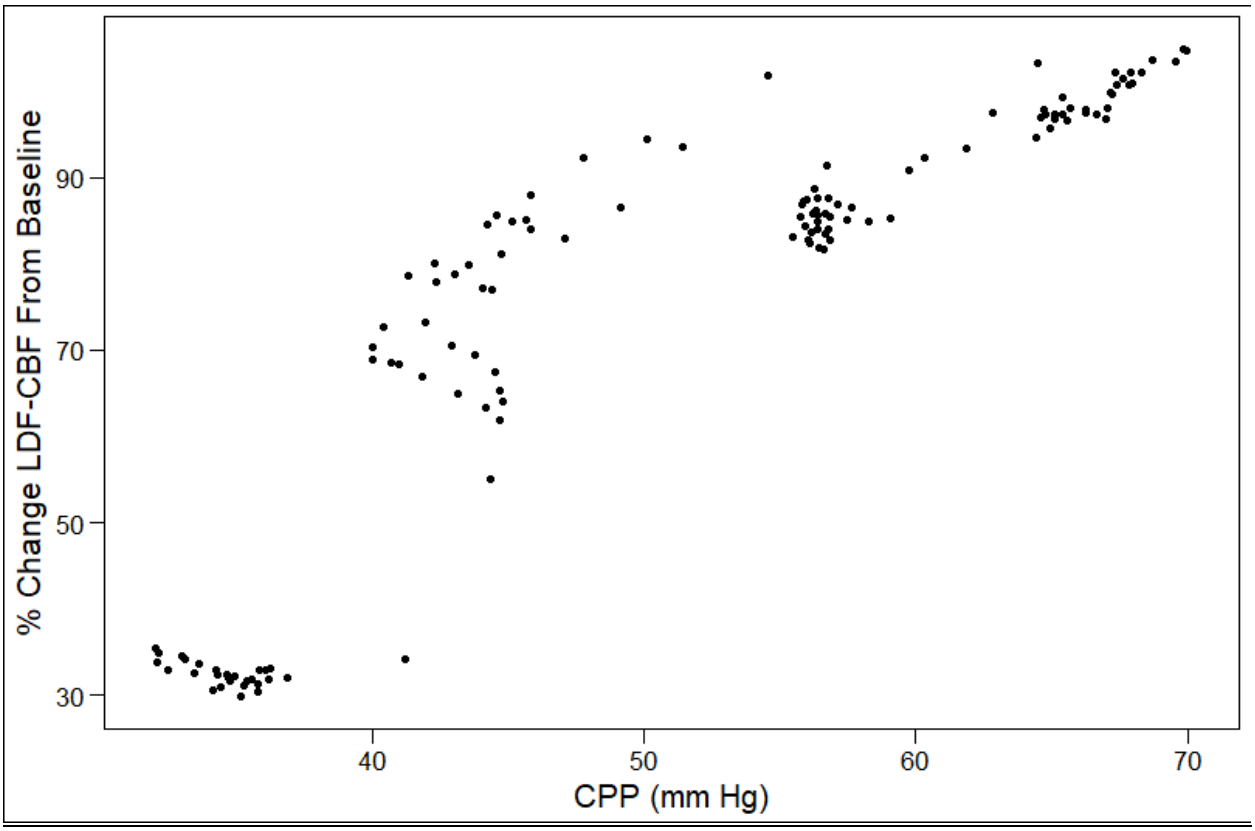
% Change LDF-CBF From Baseline
30
50
70
90
40
50
60
70
CPP (mm Hg)

12.

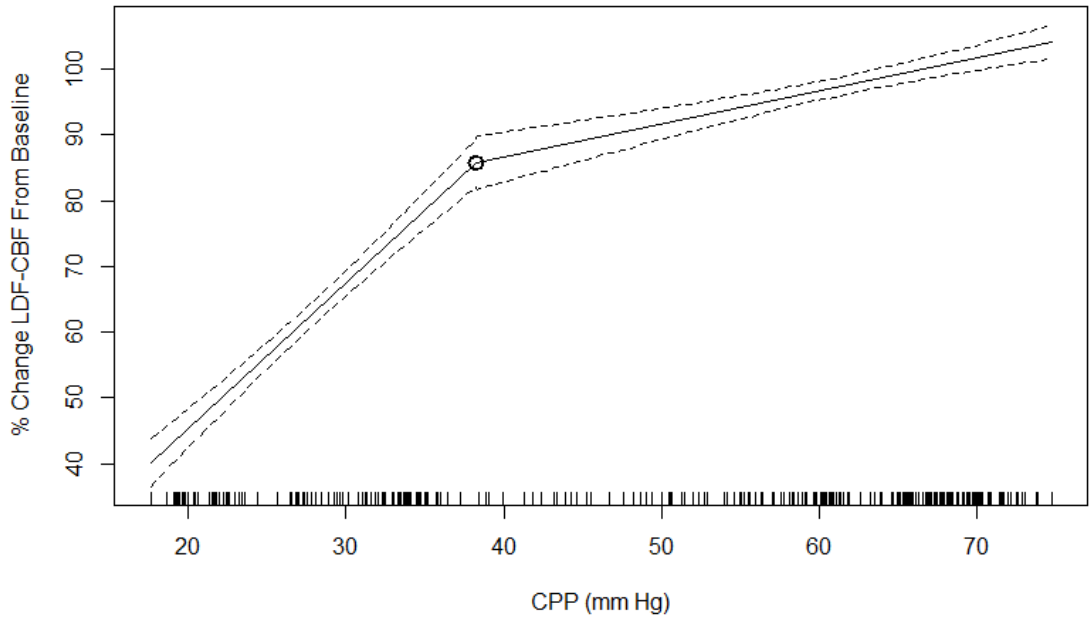
% Change LDF-CBF From Baseline
40
50
60
70
80
90
100
20
30
40
50
60
70
CPP (mm Hg)

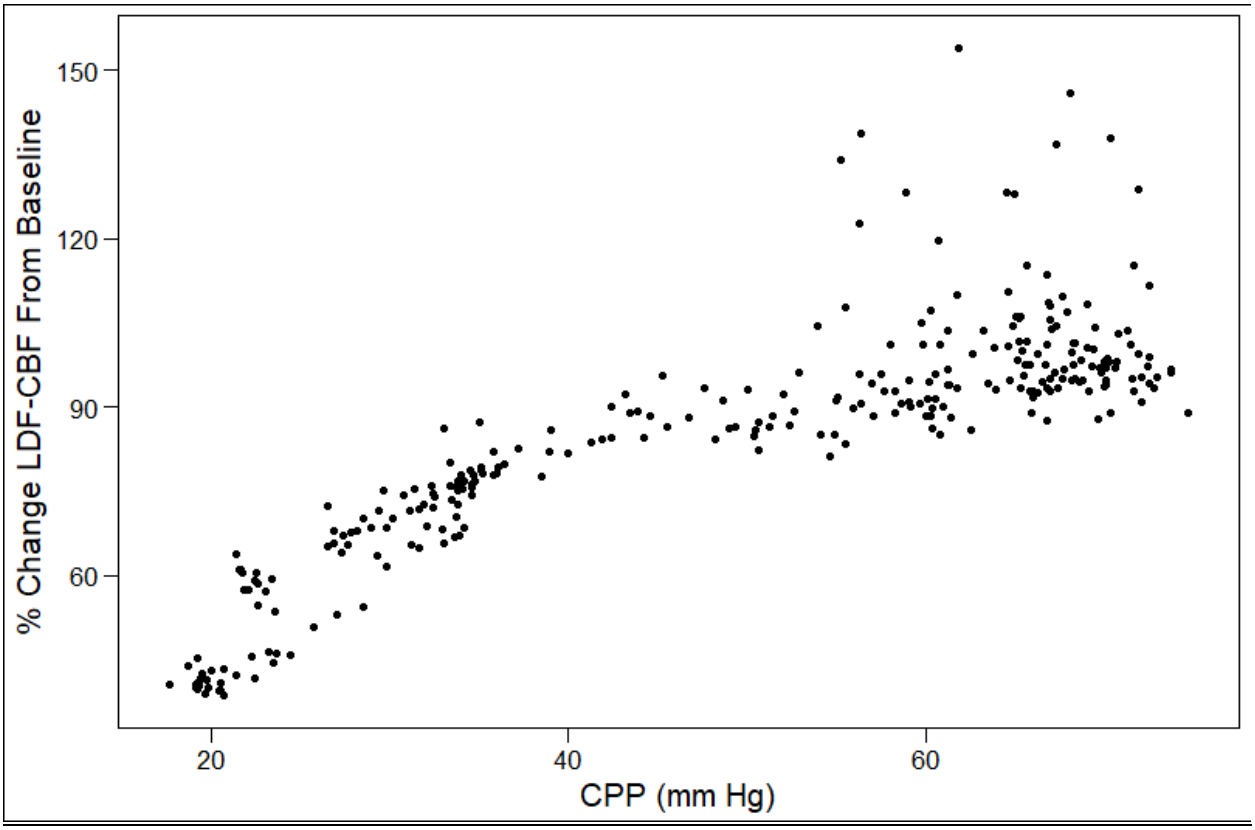
% Change LDF-CBF From Baseline
60
90
120
150
20
40
60
CPP (mm Hg)

Appendix B: CPP Versus Lx Plot

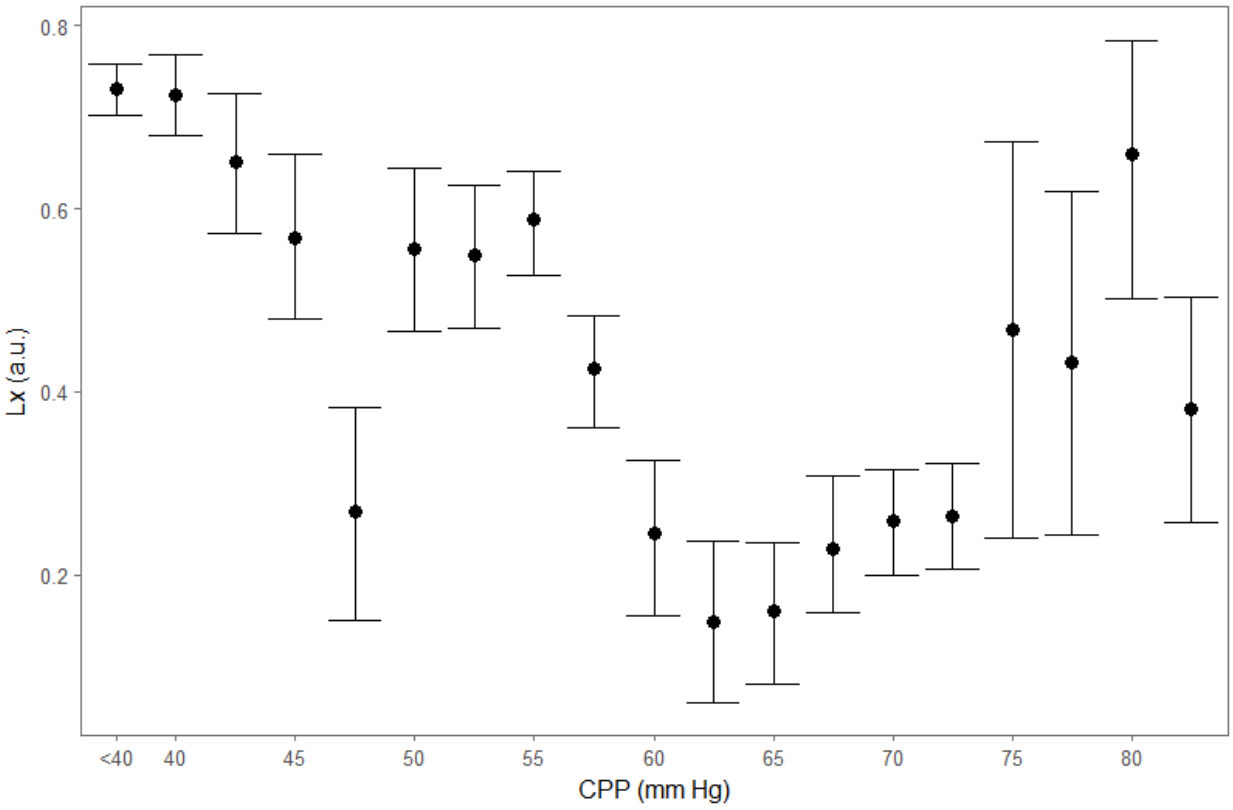

Appendix C: Bland-Altman Analysis of Index Thresholds – PRx +0.25, PAx 0, and PAx +0.25

*Bland-Altman analysis was conducted comparing the CPP at the index threshold to the CPP at the LLA, across all animals. Only the 3 index thresholds, which displayed statistically significant Pearson correlation coefficients between the CPP at thresholds and CPP at the LLA, were analyzed using Bland-Altman. All thresholds displayed poor agreement with the CPP values at the LLA.

1. PRx +0.35 Threshold

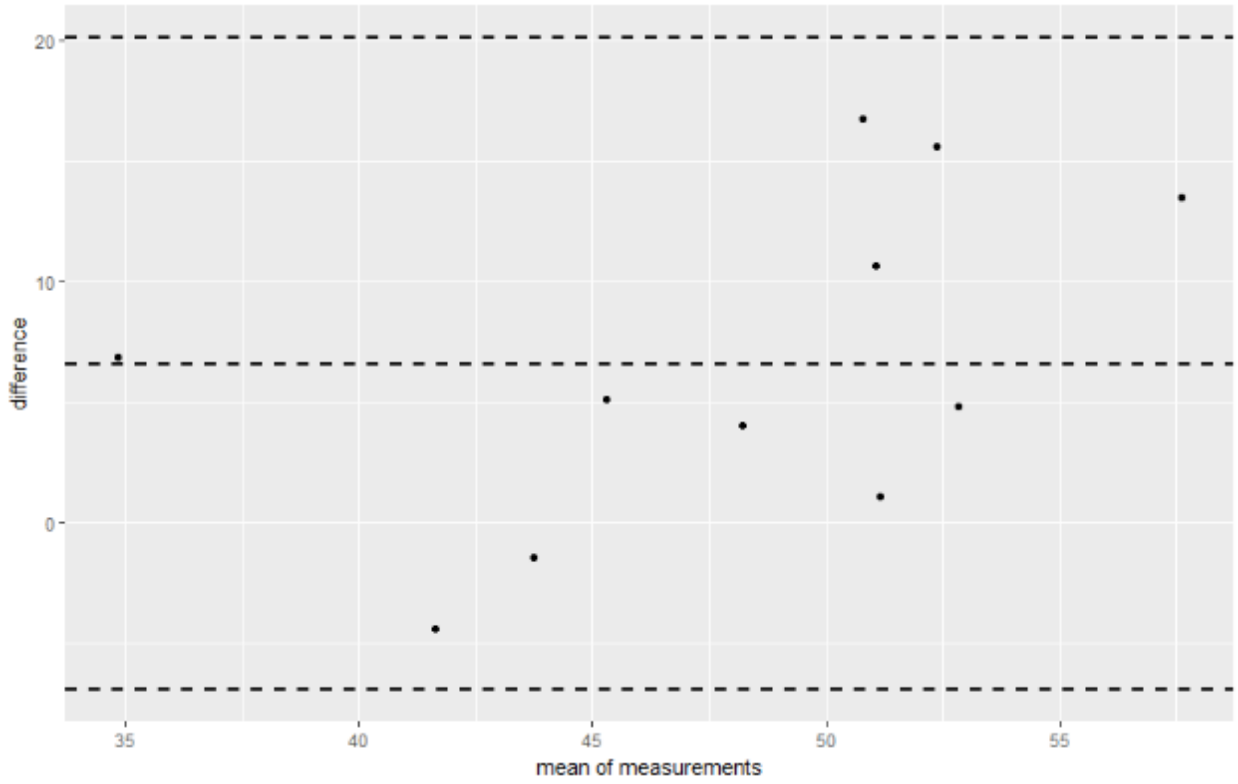


```
$lower.limit
[1] -6.942714

$mean.diffs
[1] 6.587273

$upper.limit
[1] 20.11726


critical.diff
[1] 13.52999
```

2. PAx 0 Thresholds

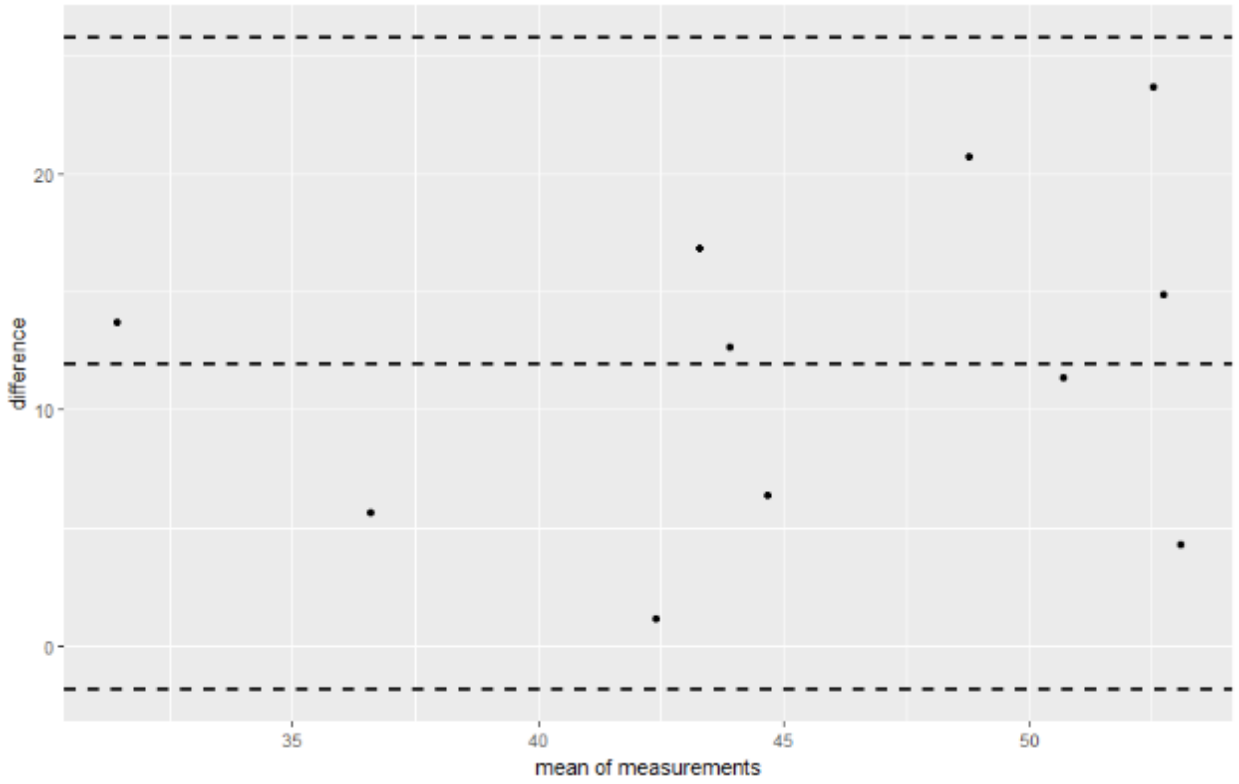


```
$lower.limit
[1] -1.833398

$mean.diffs
[1] 11.94909

$upper.limit
[1] 25.73158

$critical.diff
[1] 13.78249
```

3. PAx +0.25 Threshold

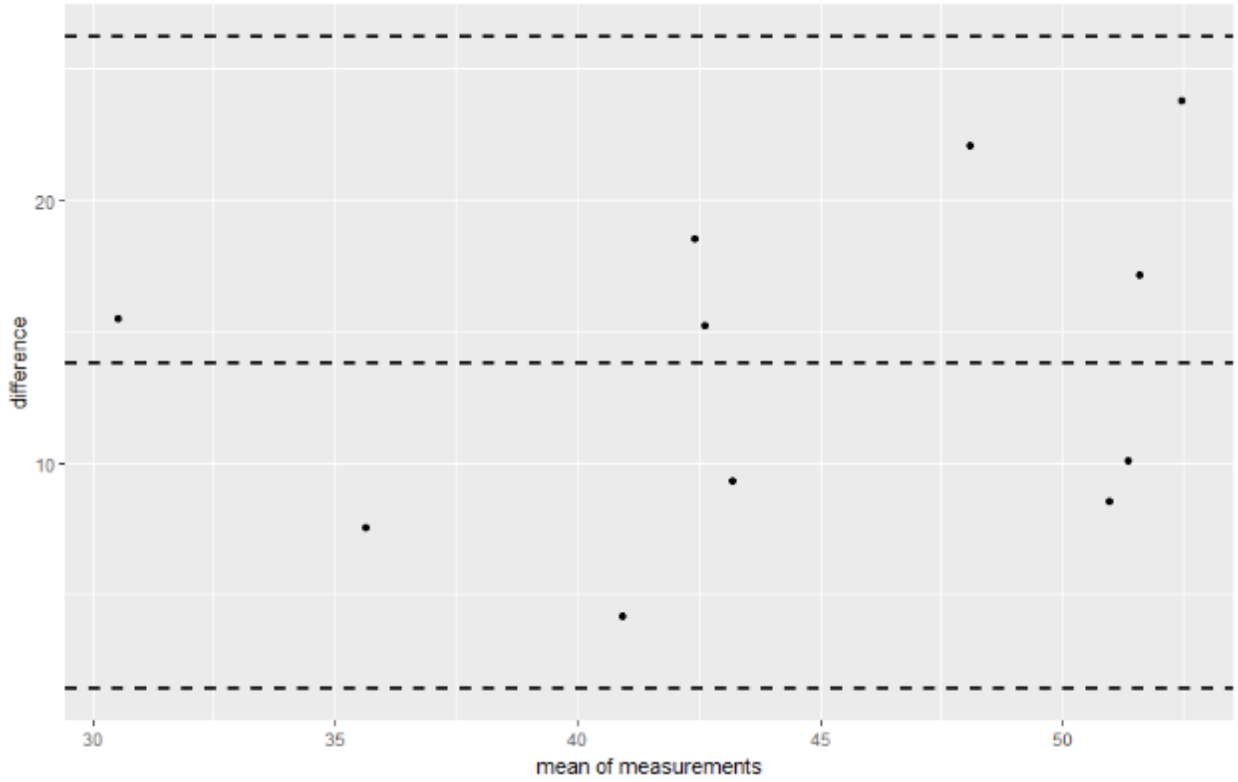


```
$lower.limit
[1] 1.420703

$mean.diffs
[1] 13.82273

$upper.limit
[1] 26.22475

$critical.diff
[1] 12.40202
```

Appendix D: ROC Curves Against the LLA for Each Continuous Index

1. PRx

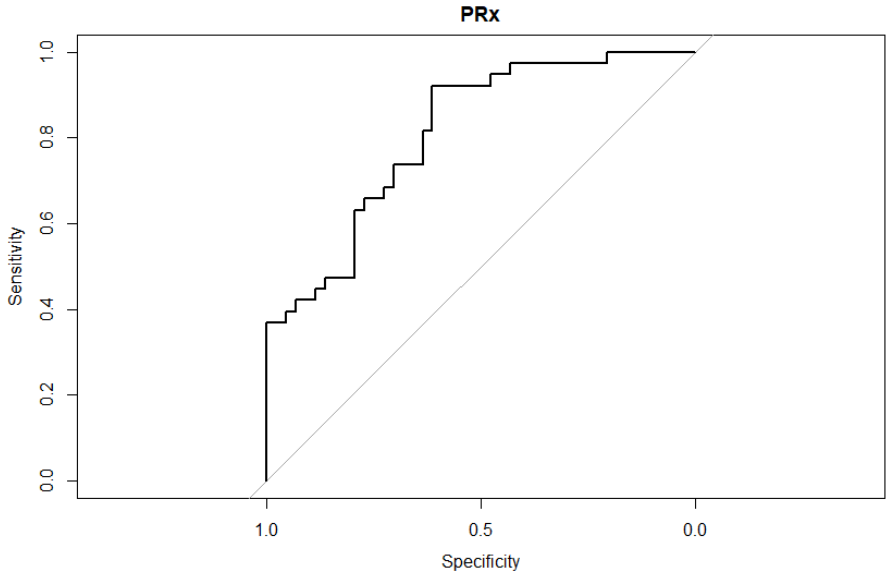

---

2. PAx

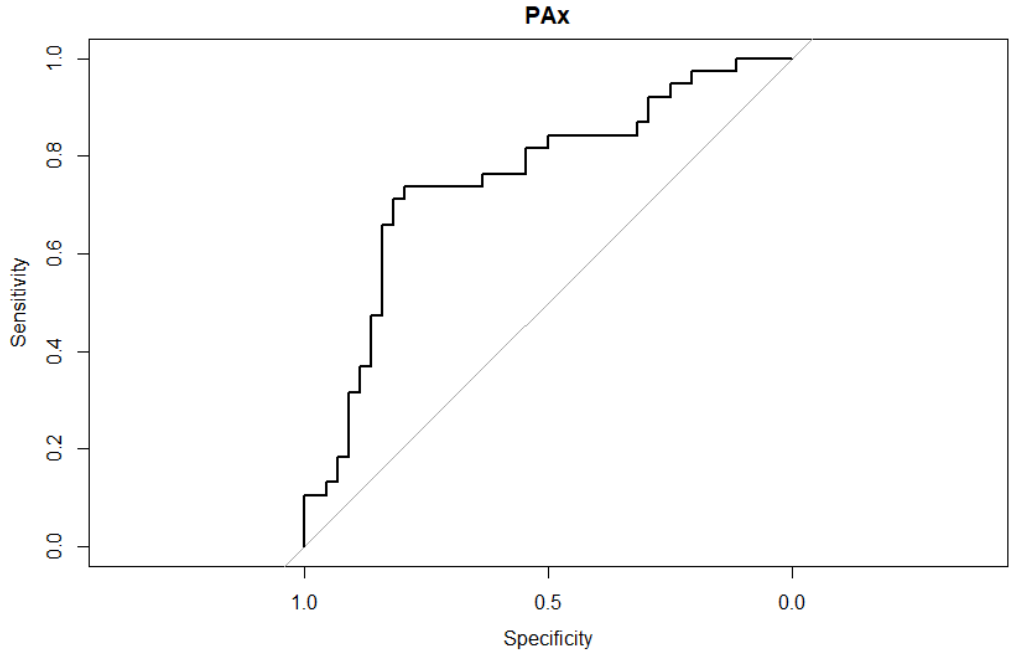

---

3. Lx

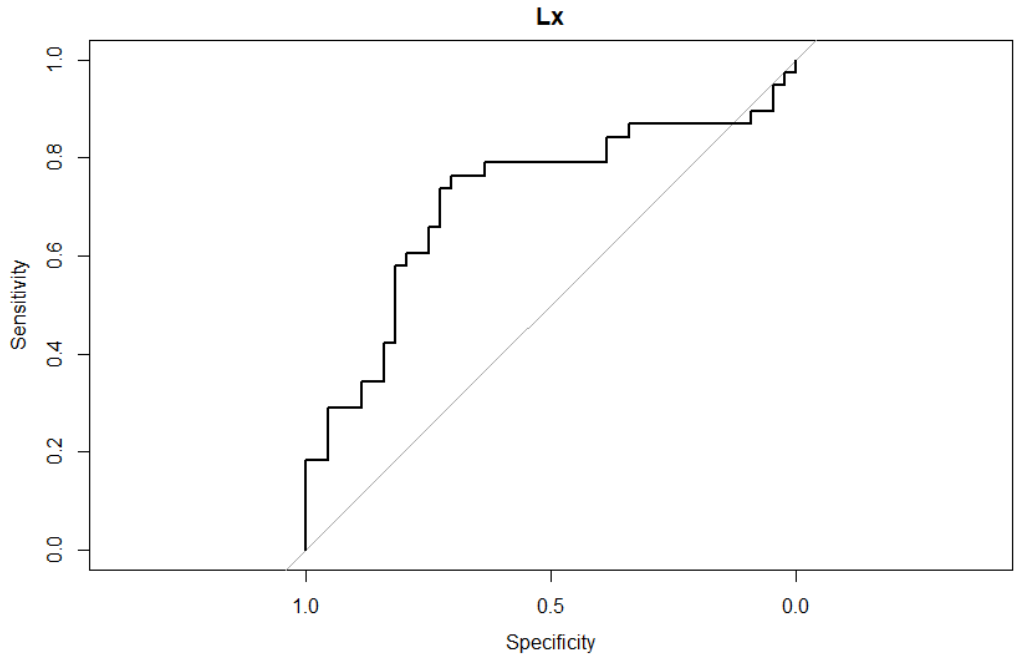

Appendix E: CPP versus AMP Error Bar Plot – Entire Cohort

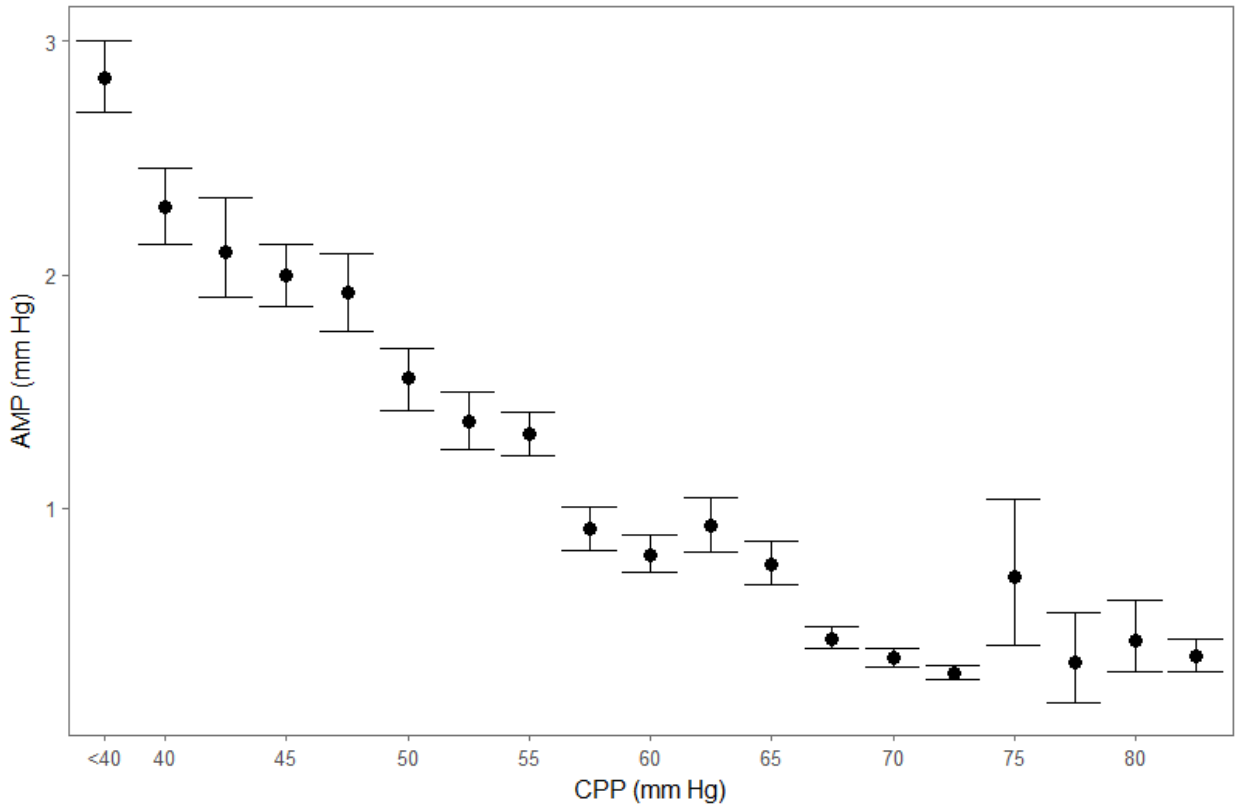

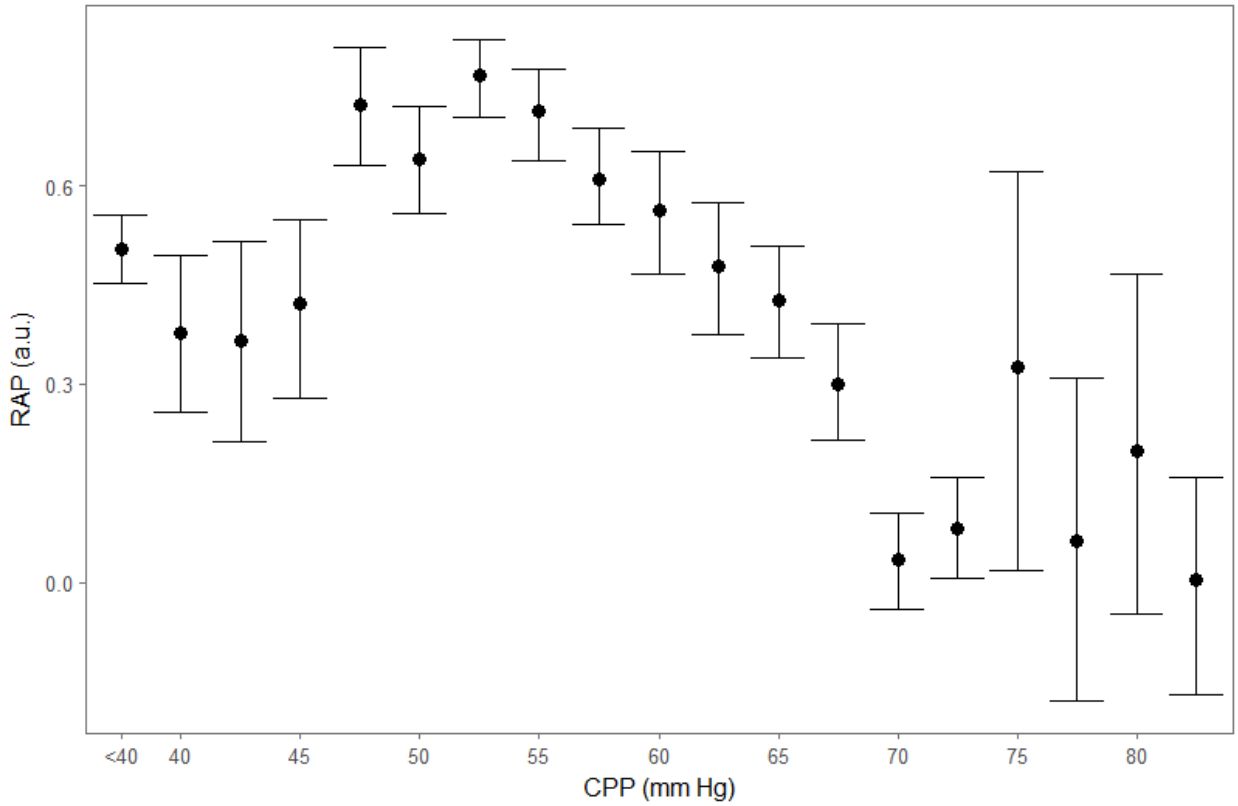
RAP (a.u.)
0.6
0.3
0.0
<40
40
45
50
55
60
65
70
75
80
CPP (mm Hg)

Appendix F: Other Indices – Error Bar Plots and ROC Analysis

1. **RAC**

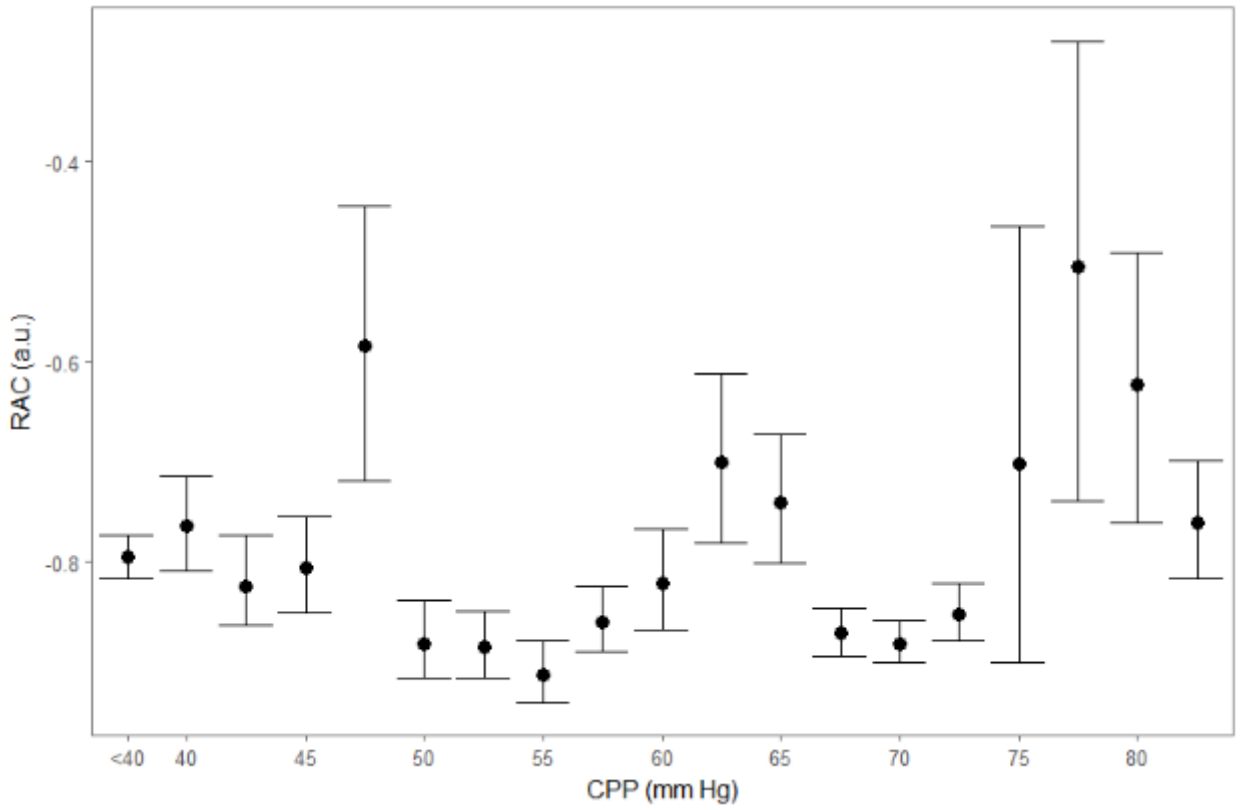

ROC Analysis:

Area under the curve: 0.5575
95% CI: 0.478-0.6371 (DeLong)

P = 0.325

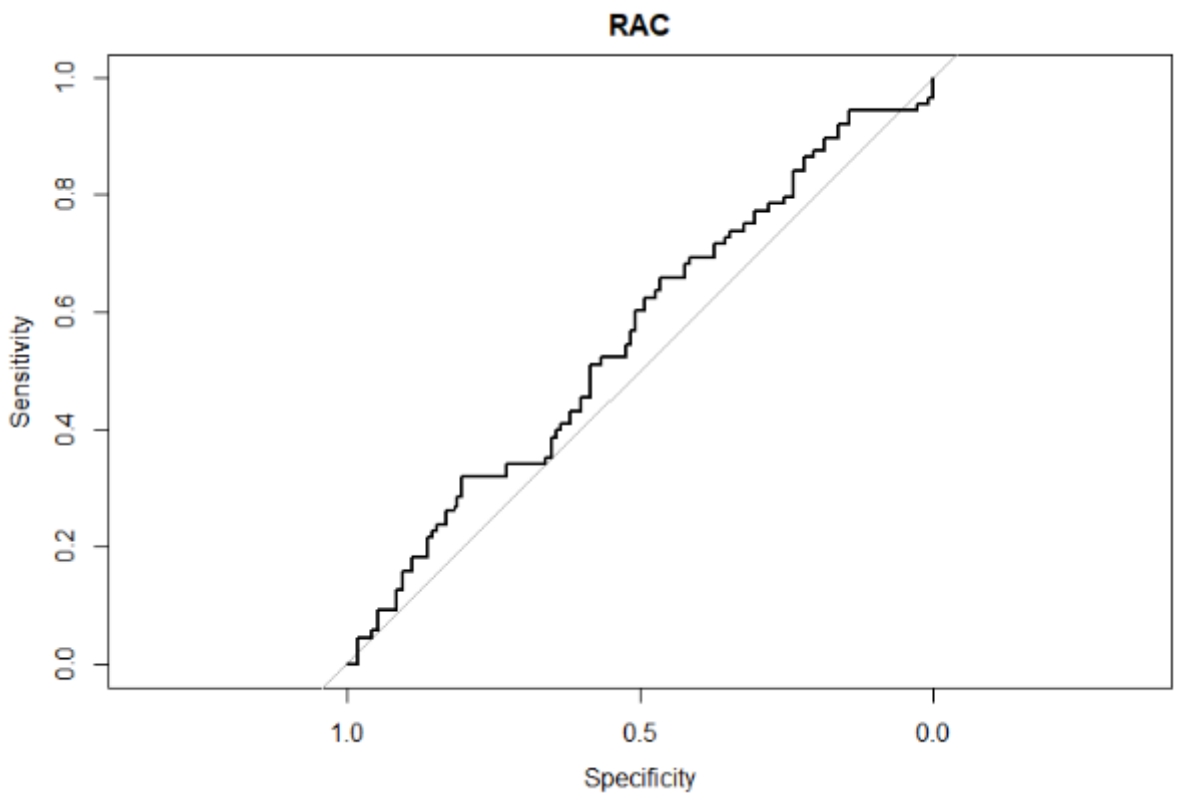
RAC
Sensitivity
0.0
0.2
0.4
0.6
0.8
1.0
1.0
0.5
0.0
Specificity

2. **Mx**

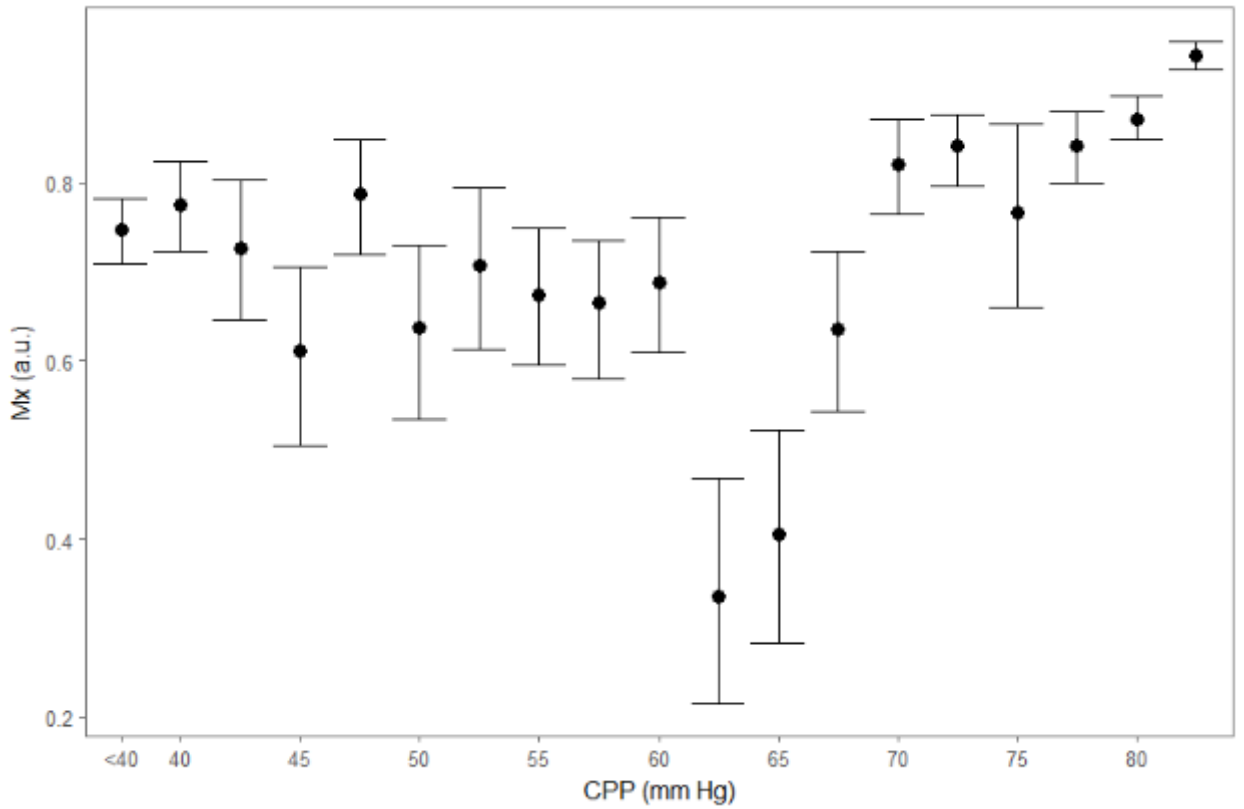

ROC Analysis:

Area under the curve: **0.5381**
95% CI: 0.4586-0.6177 (DeLong)

P = 0.408

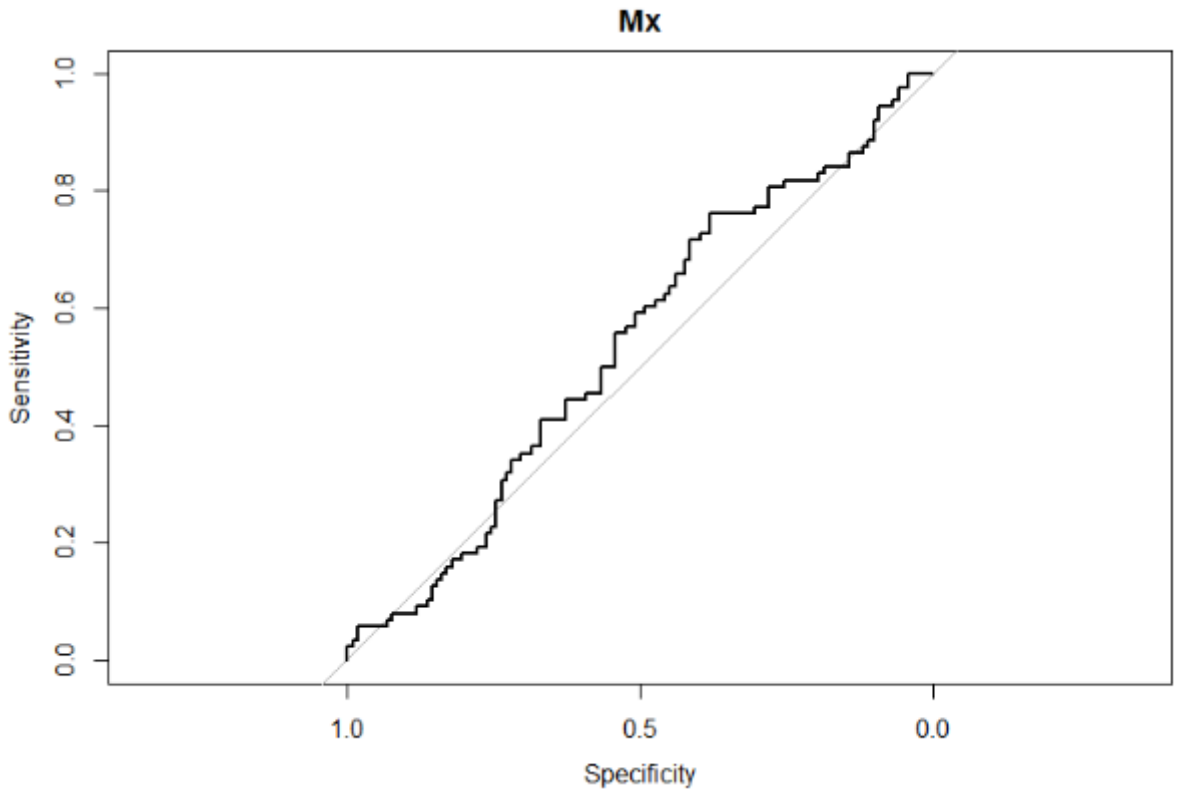
Mx
Sensitivity
0.0
0.2
0.4
0.6
0.8
1.0
1.0
0.5
0.0
Specificity

3. **Sx**

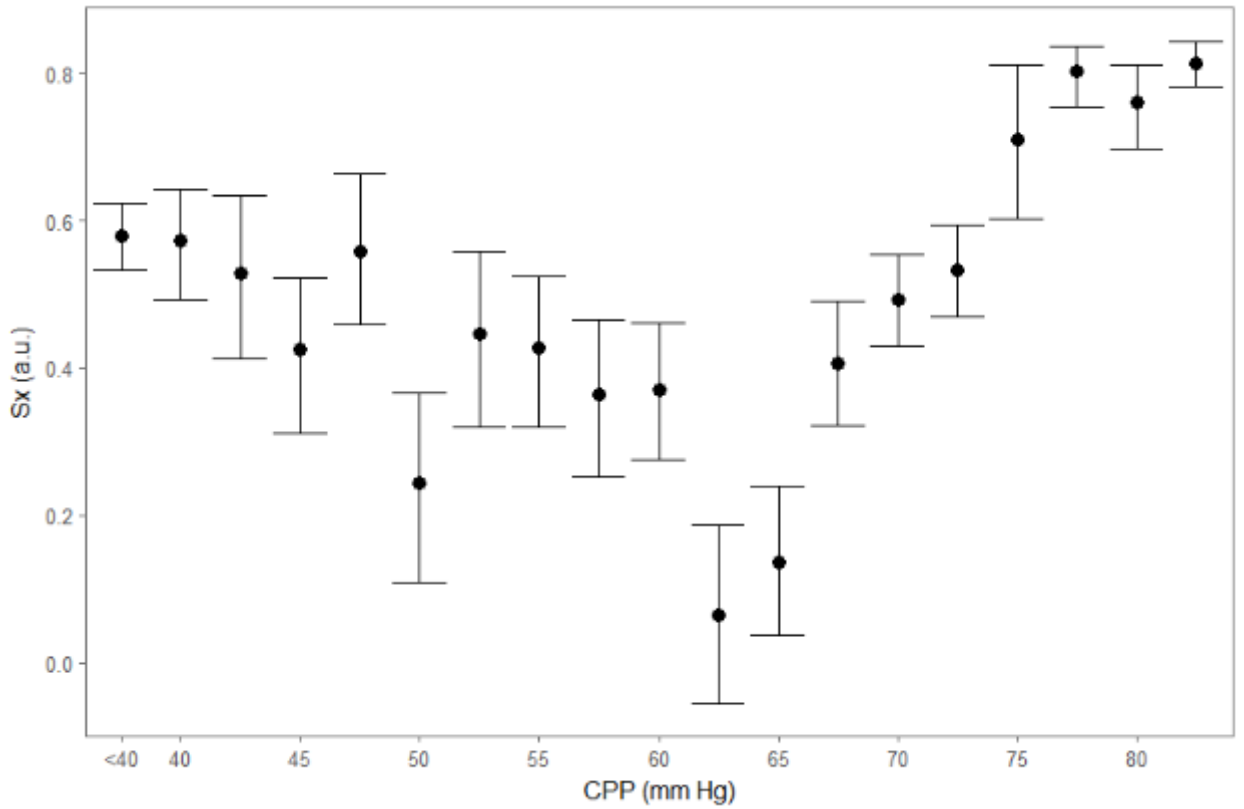

ROC Analysis:

Area under the curve: **0.5872**
95% CI: 0.5078-0.6665 (DeLong)

P = 0.086

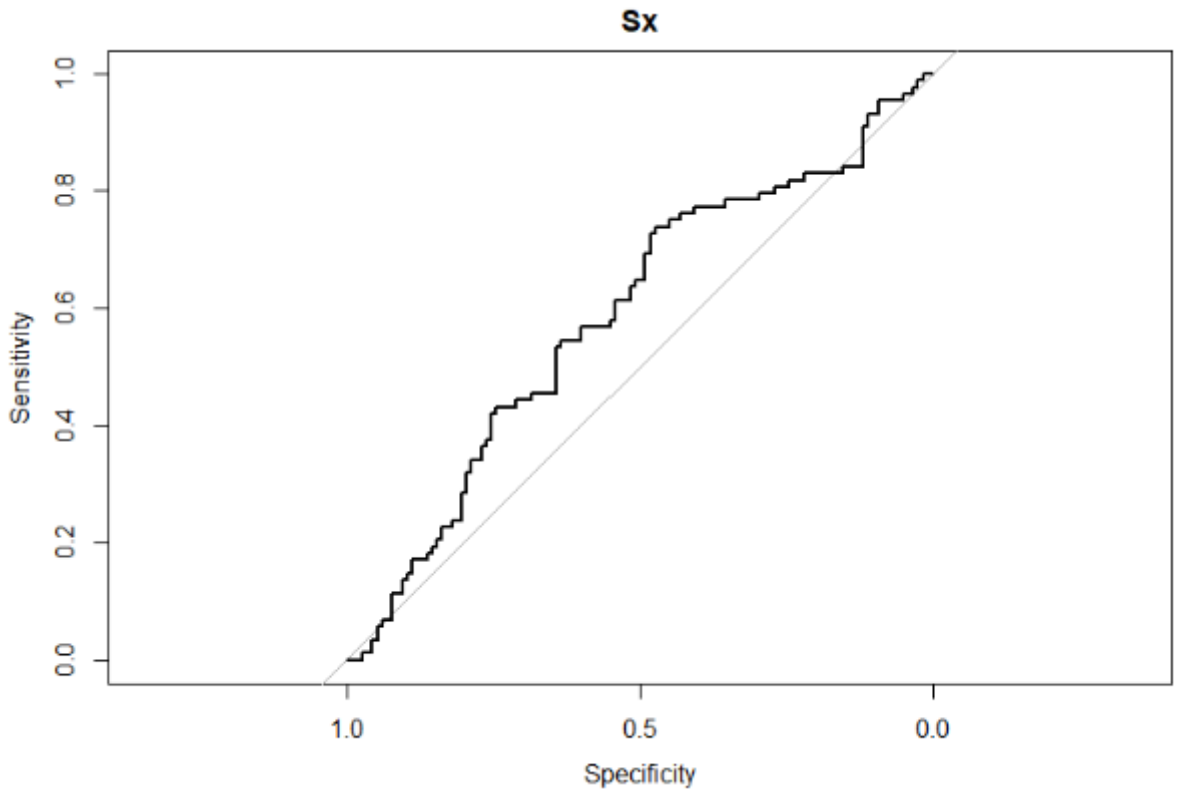
Sx
Sensitivity
0.0
0.2
0.4
0.6
0.8
1.0
1.0
0.5
0.0
Specificity